2011-01-01

Development of a Heat Transfer Test Rig for Finding Heat Transfer Characteristics of Liquid Methane

Sergio Flores
University of Texas at El Paso, sergio.flores86@gmail.com

DEVELOPMENT OF A HEAT TRANSFER TEST RIG FOR FINDING HEAT TRANSFER CHARACTERISTICS OF LIQUID METHANE

SERGIO FLORES

Department of Civil Engineering

APPROVED:

_____
Ahsan Choudhuri, Ph.D., Chair

_____
Cesar Carrasco, Ph.D.

_____
Norman Love, Ph.D.

_____
Benjamin Flores, Ph.D.
Acting Dean of the Graduate School

This thesis is dedicated to my family and fiancée for all their love and support

DEVELOPMENT OF A HEAT TRANSFER TEST RIG FOR FINDING HEAT TRANSFER CHARACTERISTICS OF LIQUID METHANE

by

SERGIO FLORES, B.S. Architectural Engineering

THESIS

Presented to the Faculty of the Graduate School of

The University of Texas at El Paso

in Partial Fulfillment

of the Requirements

for the Degree of

MASTER OF SCIENCE

Department of Civil Engineering

THE UNIVERSITY OF TEXAS AT EL PASO

December 2011

ACKNOWLEDGEMENTS

There are certain people who deserve credit for all their help and guidance throughout the entire project and the writing of this thesis. I would like to thank the PhD students, who served as sub-advisors, Adrian Trejo and Chance P. Garcia for their knowledge and expertise which served a large role in making the experiment possible. I also want to thank Manuel Galvan for his assistance during experimentation. A special thanks goes to National Aeronautics and Space Administration (NASA) for funding this research and the Associate Director of cSETR Nathaniel Robinson and research advisor Dr. Ahsan Choudhuri for their direction in the project. The funding for this thesis was suported by NASA under award No(s) NNX09AV09A.

ABSTRACT

Most large scale rocket engines use a regeneratively cooled system to cool the rocket engine using either the rocket's fuel or oxidizer. The use of liquid methane as a rocket fuel is an emerging technology proving to have several advantages over current rocket fuels. However, liquid methane is lacking the extensive research as a rocket fuel compared to highly used rocket fuels like liquid hydrogen. A heat transfer test rig was built with the goal to characterize the heat transfer characteristics of liquid methane as it passes through a heated channel. The development of the test rig underwent considerations designed to replicate the conditions in a regenerative cooling channel. Experiments were first completed using liquid nitrogen in vacuum resulting in temperature data which show evidence of boiling in the channel causing vapor lock.

TABLE OF CONTENTS

ACKNOWLEDGEMENTS ……. v

ABSTRACT ……...……...vi

TABLE OF CONTENTS ……vii

LIST OF FIGURES …….....ix

LIST OF TABLES ……x

Chapter

1. INTRODUCTION ……..… 1

1.1 Introduction ……..…… 1

1.2 Problem Statement ……...… 1

1.3 Objectives ……..... 2

2. LITERATURE REVIEW …….. 3

2.1 Liquid Methane ……..... 3

2.2 Regenerative Cooling …….……..… 4

2.3 Earlier Study …… 4

3. EXPERIMENTAL SETUP …...……. 6

3.1 Experimental Equipment …….……... 6

3.1.1 Vacuum Chamber ……..… 6

3.1.2 K-Type Thermocouples ……...…....…. 7

3.1.3 Heating Cartridges …….…….... 8

3.1.4 Solid State Relays …….…… 9

3.1.5 Temperature Controller ……... 10

3.1.6 Data Acquisition System ……..... 11

3.1.7 Cryogenic Globe Valve ……...…… 12

3.2 Experimental Design and Setup …….……...……. 13

3.2.1 Rig Design …….. 13

3.2.2 Flow Rate …….……...…… 16

4. RESULTS ……..…….. 18

4.1 Radiation and Heat Flux…….…… 18

4.2 Liquid Nitrogen Test Results and Analysis …….…….. 20

4.3 Liquid Methane Test Results and Analysis ……... 25

5. CONCLUSIONS ……. 28

5.1 Conclusions …… 28

5.2 Recommendations and Future Work …….……...…. 28

REFERENCES ……...…. 30

APPENDIX ……...…… 31

Appendix A: Rig Development …….…….. 31

Appendix B: Channel Wall Temperature with Time Plots…….. 32

Appendix C: Channel Wall Temperature with Distance Plots……. 35

Appendix D: Channel Wall Temperature with Distance Normalized Plots …...…..…… 37

Appendix E: Liquid Methane Tests ……...…...… 40

CURRICULUM VITAE …….. 42

LIST OF FIGURES

Figure 1. The original and improved test section configurations ……..… 5
Figure 2. Stainless steel vacuum chamber ……..… 7
Figure 3a. K-Type thermocouples (14 gage) with ceramic insulation ……... 8
Figure 3b. K-Type thermocouples with threaded end ……..…. 8
Figure 4. Cartridge heaters with ¼” (0.64 cm) diameter and 5” (13 cm) length ……...… 9
Figure 5. Five solid state relays attached on aluminum plate, Omega.com ……..… 10
Figure 6. Temperature Controller with digital interface ……...… 11
Figure 7. DAQ system with 16 ports connected to the computer via USB ……..… 11
Figure 8. DAQ for pressure transducers ……...… 12
Figure 9. Cryogenic globe valve ……...… 13
Figure 10. Assembled heating block ……...…. 14
Figure 11. Assembled cooling channel with thermocouples ……...…. 16
Figure 12. Heat flux at 891 kW/m^2 [0.545 Btu/s-in^2], wall temperature ……. 21
Figure 13. Heat flux at 891 kW/m^2 [0.545 Btu/s-in^2] normalized plot …… 21
Figure 14. Channel with vapor on the channel wall at TC4, TC5, and TC6 ……...… 22
Figure 15. Average coolant side wall temperature compared to heat flux ……..…. 24
Figure 16. Entire heat rig system setup for testing ……...… 25
Figure 17. First LCH_4 test at heat flux 3743 kW/m^2 (1.85 BTU/s-in^2), wall temperature …….. 26
Figure 18. Second LCH_4 test at heat flux 3743 kW/m^2 (1.85 BTU/s-in^2), wall temperature ….. 26
Figure 19. Legend of schematic piping ……...… 30
Figure 20. Phase 1 of schematic with methane production ……..…… 30
Figure 21. Phase 2 of schematic with run tank …… 31

LIST OF TABLES

Table 1. Fuel flow rate determined from designed thrust in a rocket engine …….. 17
Table 2. Heat Rig Radiation Loss …… 19
Table 3. Heat flux using radiometer …… 19
Table 4. Calculated and Experimental Heat Flux Loss ……... 20
Table 5. Inlet Pressure and Estimated Flow Rate …… 23

Chapter 1

INTRODUCTION

1.1 Introduction

Liquid methane is being considered for use as a fuel in rocket engines. At the time of this thesis, little is known of the fluid heat transfer properties of liquid methane in comparison to the more commonly used rocket fuels like liquid hydrogen. This thesis focuses on the design and development of the Center for Space Exploration Technology Research (cSETR) rig built to find the heat transfer characteristics of liquid methane. In modern rocket engines the fuel and sometimes oxidizer is used for cooling the material of the rocket by means of cooling channels; this method is known as regenerative cooling. The cSETR rig uses a heated channel designed to replicate the conditions experience in a regeneratively cooled channel. Regeneratively cooled rocket engines use rocket fuel during the operation of a rocket to allow for cooling of the engine material; this prevents the material from failing due to melting under the extreme temperatures of the rocket during combustion [1]. The fuel runs through channels inside the nozzle from the nozzle end to the injector [2].

1.2 Problem Statement

An experimental heat transfer testing rig was designed and built by cSETR to simulate a cooling channel in a regeneratively cooled rocket system using liquid nitrogen (LN_2) and liquid methane (LCH_4) as the coolant. The Air Force Research Laboratory, Propulsion Directorate at Edwards Air Force Base in California has designed a ‘carbothermal’ test rig to conduct similar experiments using RP-2 as the coolant [3]. Carbothermal refers to the use of carbon at elevated

temperatures. Investigating the use of LCH_4 as a rocket fuel has risen from the need to find a more abundant and green fuel for use in rockets. The heat transfer test rig

1.3 Objectives

The goal of this thesis is to explain the design and development of the experimental heating rig created by the cSETR at the University of Texas at El Paso (UTEP). The design covers the concept behind the heating rig, materials and parts chosen, as well as tests done on the rig to prepare it for experimenting on LCH_4. The testing done includes heating tests, measuring heat flux loss due to radiation, and LN_2 tests.

Chapter 2

LITERATURE REVIEW

2.1 Liquid Methane

The use of liquid methane as a fuel in rocket engines is an emerging technology. Currently the documented work on the thermal properties of liquid methane is not as abundant as a common rocket fuels like liquid hydrogen. There are many advantages that make methane a promising candidate as a rocket fuel. The melting point and density of LCH_4 are both higher than that of liquid hydrogen allowing for smaller storage tanks minimizing the weight and space required for storage. When comparing a previously used fuel such as kerosene, which is a close chemical hydrocarbon to liquid methane, the specific impulse of liquid methane in vacuum is about 370 seconds to kerosene's vacuum specific impulse of about 355 seconds [4]. Liquid methane has also been found to have low pressure drops in cooling channels, exceptional cooling capabilities, and coking at higher points with less soot [5].

The inclusion of a LCH_4 production tank was essential in the development of the cSETR heat transfer rig experiment due to the lack of pure LCH_4 suppliers in the area. Using liquid natural gas instead of LCH_4 would run the risk of impurities causing unrepeatable results. The LCH_4 production tank was designed as a heat exchanger. The tank was built to hold low pressurized gaseous methane while LN2 is run through a coil inside the tank. The temperature of liquid nitrogen (77 K) is lower than the temperature of liquid methane (112 K) allowing for the gaseous form of methane to condense when coming in contact with the coil with liquid nitrogen.

2.2 Regenerative Cooling

Regenerative cooling is one of several methods of cooling a rocket engine such as dump cooling, film cooling, transpiration cooling, ablative cooling, and radiation cooling [1]. In regenerative cooling method the rocket fuel serves as a coolant which flows through a series of reinforced tubes that make up the wall of the rocket. The coolant travels to the end of the rocket gathering energy then it makes its way into the injector for combustion [2]. Some of the advantages of this system include reusable coolant (injector reuses the coolant), light weight construction compared to other systems, and it allows for long firing times. Some of the disadvantages to using this system are lower reliability with certain coolants and the 'maximum allowable coolant temperature' can put limits on parameters in the design such as mixture ratio and nozzle area ratio [1].

2.3 Earlier Study

The Air Force Research Laboratory (AFRL) Propulsion Directorate designed a high heat test rig to investigate the 'thermal performance' of RP-2. The AFRL used cartridge heaters to heat a copper block which was then used to conductively heat a copper channel in vacuum. An electrically heated channel runs can cause erroneous data when taking thermocouple measurements. When designing the shape of the copper block, they found that in the interface between the channel and the copper block there is "improved performance" when inserting a groove on the block allowing the channel to lie directly on the copper block [3]. Through this method the copper block directly heats the channel without the need to heat another medium before reaching the channel. Figure 1 shows the cross section of two configurations considered by the AFRL Propulsion Directorate. The picture on the left in Figure 1 shows the original

configuration of the AFRL setup while the picture on the right shows the modified configuration. Figure 1 shows the cross-sectional view of the channel and heating block with the channel going into the page.

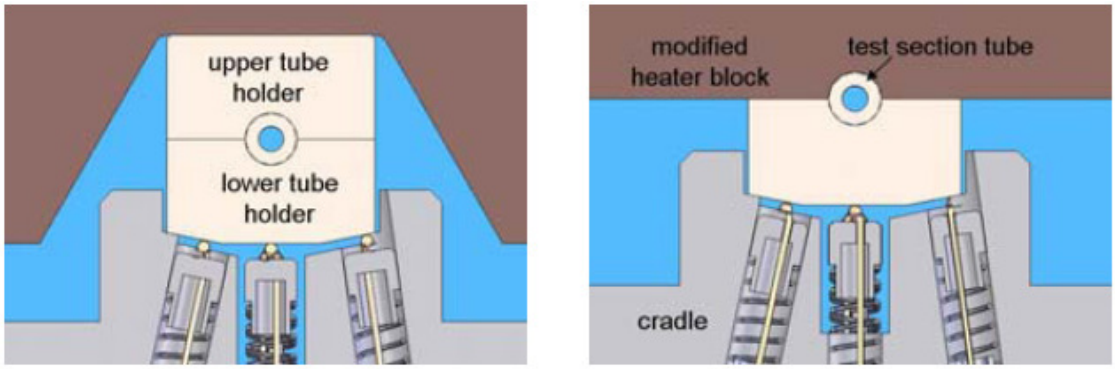

Figure 1. The original and improved test section configurations [modified from reference 2].

It is important in the cSETR experiment to have the flexibility of using different channel shapes and sizes for flexibility in future work. The AFRL design, however, does not allow for different shaped channels to lie flush on the groove of the block once a groove has already been machined. A separate heating block would have to be made for every different sized channel. For this reason, the experiment conducted by the cSETR uses a test section like the picture on the left in Figure 1. The test section holds the channel without having to modify the copper block but by modifying the test section instead. In the cSETR test rig, liquid nitrogen and liquid methane were investigated using a cooling channel test rig comparable to that of the experiment conducted by the AFRL Propulsion Directorate.

Chapter 3

EXPERIMENTAL SETUP

3.1 Experimental Equipment

This part of the chapter explains the equipment used in the development of the heat transfer rig.

3.1.1 Vacuum Chamber

A vacuum chamber was used for the experiment to obtain results closer to simulate the conditions of a rocket regenerative cooling channel operating in the vacuum of space. When operating in a vacuum there are no convective heat losses to cool down the heating block; the heating block will only suffer heat losses due to radiation. In the vacuum chamber, two vacuum feedthroughs were custom made to allow for K-type thermocouples and electrical wiring to get through the vacuum without compromising the vacuum in the chamber. The vacuum feedthroughs are connected to the vacuum chamber with a CF flange. A picture of the vacuum chamber used can be seen in Figure 2 along with the two different feedthroughs.

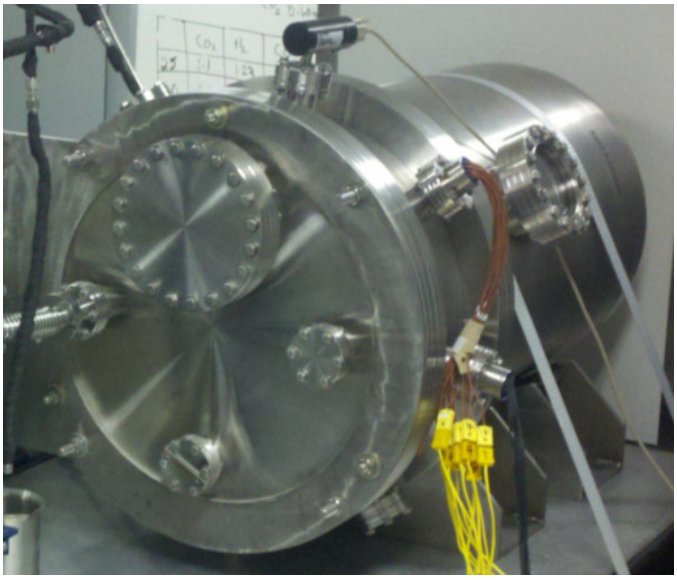

Figure 2. Stainless steel vacuum chamber.

The vacuum chamber reached pressure conditions of 0.07 torr (9.3 Pa).

3.1.2 K-Type Thermocouples

The K-Type thermocouples in the experiment were used to measure the temperature on the copper block, the channel in the test section, and the temperature on the stainless steel piping. There were 6 thermocouples placed on the channel to record temperature data with time. An additional five thermocouples were placed around the block to control the temperature of the block as it reached the desired point. To make sure there was liquid running through the lines, two thermocouples were positioned on the stainless steel lines prior to entering the heating block. According to the thermocouple manufacturer, Omega Engineering Inc., the K-Type thermocouples that were used on the heating block are insulated with a ceramic rated to 1200 °C (2192 °F). All the K-type thermocouples have a working temperature range of -185 to 1250 °C (-302 to 2282 °F). The large temperature range is essential for the reading the heating block temperatures and the below freezing temperatures both found in the experiment. The

thermocouples transferred data outside the vacuum chamber through the vacuum feedthroughs. The two different types of thermocouples can be seen in Figure 3a and 3b.

Figure 3a. K-Type thermocouples (14 gage) with ceramic insulation, from Omega.com.

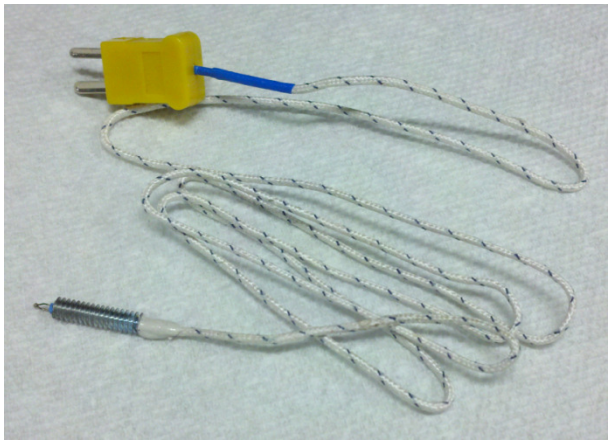

Figure 3b. K-Type thermocouples with threaded end.

An E-type thermocouple was placed inside the methane production tank through the bore-through Swagelok fitting. E-type thermocouples have a higher output thank K-type making them stable for reading cryogenic temperatures.

3.1.3 Heating Cartridges

The experiment consists of 21 heating cartridges that can reach a temperature of 1200 °C (1292°F). The heating cartridges are electrically heated and are used provide the heat source

required to elevate the temperature of the copper heating block. In the same way the thermocouples entered the vacuum chamber, the heating cartridges received power through electrical wires going through the custom, vacuum rated CF flanges. A picture of the heating cartridges can be seen in Figure 4. Each heating cartridge provides 400W of power with a heat flux of 178 kW/m^2.

Figure 4. Cartridge heaters with ¼" (0.64 cm) diameter and 5" (13 cm) length, from Omega.com.

3.14 Solid State Relays

Two types of solid state relays were used, two 50A and three 25A, to send power and a signal to the heating cartridges. The heating cartridges can be controlled by the temperature controller in conjunction with the solid state relays to turn the heaters on and off. In the experiment five solid state relays were used to control all the attached heating cartridges. Each relay used its own power source. Figure 5 shows a picture of the solid state relays.

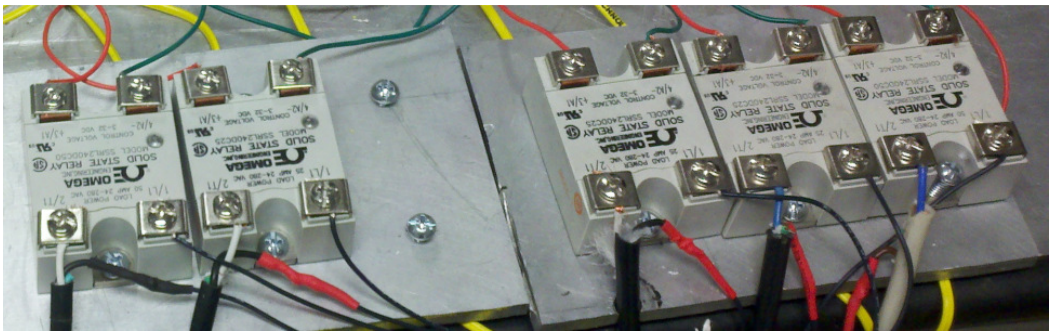

Figure 5. Five solid state relays attached on aluminum plate, Omega.com.

3.1.5 Temperature Controller

The temperature controller has six zones for thermocouple input and six zones for solid state relay input. It has the ability of controlling the temperature at which the heating cartridges will stop heating by using the thermocouples as a reference temperature. Since the previously mentioned heating cartridges have a working temperature of about 1200 °C, it is necessary to set a temperature so that the heating cartridges do not burn out. In the experiment, the temperature controller is linked to a computer via an RS-232 cable, this allows for data to be transmitted directly to the computer using the temperature controller software. Only five of the six zones were used. Figure 6 shows a picture of the temperature controller with the connections exiting the back. A power supply was attached as an input to the temperature controller to provide the necessary output of 5 V that are required to activate the solid state relays.

Figure 6. Temperature Controller with digital interface, Omega.com.

3.1.6 Data Acquisition Systems (DAQ)

The thermocouple DAQ consists of 16 channels allowing for maximum placement of 16 thermocouples. Temperature data was recorded using this DAQ for the inlet line temperature of the fluid and the temperature profile along the cooling channel. The sample rate of the DAQ is 1200 samples per second. The DAQ can be seen in Figure 7 with the thermocouples attached on the right (yellow cables) and the usb port on the left (black). A total of 11 slots were used from this DAQ, 6 thermocouples for the channel, 4 thermocouples on the line before and after the channel, and one thermocouple for the methane production.

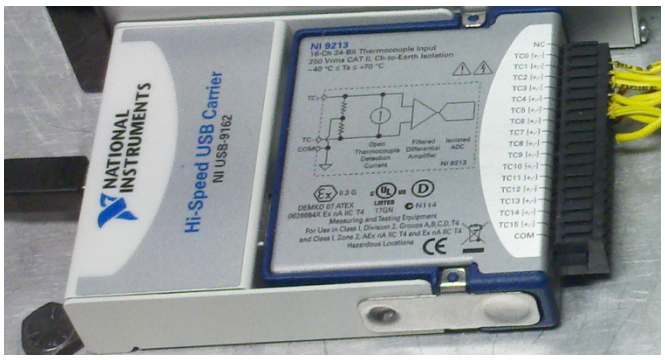

Figure 7. DAQ system with 16 ports connected to the computer via USB, National Instruments.

A separate DAQ was used to record pressures from the pressure transducers and the readings from the radiometer, Figure 8. Using a Labview program, the thermocouple readings were recorded simultaneously with the readings from the pressure transducers both with a frequency of 10 Hz; the radiometer readings also used the same program with the same frequency.

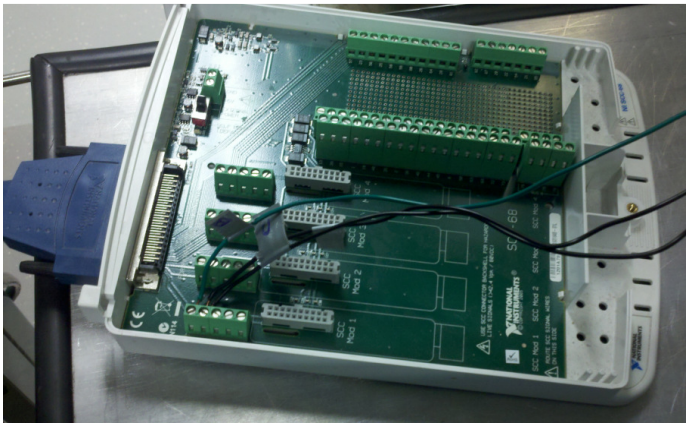

Figure 8. DAQ for pressure transducers, National Instruments.

3.1.7 Cryogenic Globe Valve

The manual turn valves used in the gas piping run the risk of freezing shut when used while running cryogenic fluids; for that reason, a cryogenic globe valve was used before and after the liquid methane storage tank. At this location it is important the valve can open and close without malfunctioning to allow for the liquid methane to exit the storage tank. This globe valve can operate at temperatures as low as 74 K with pressures up to 5 MPa.

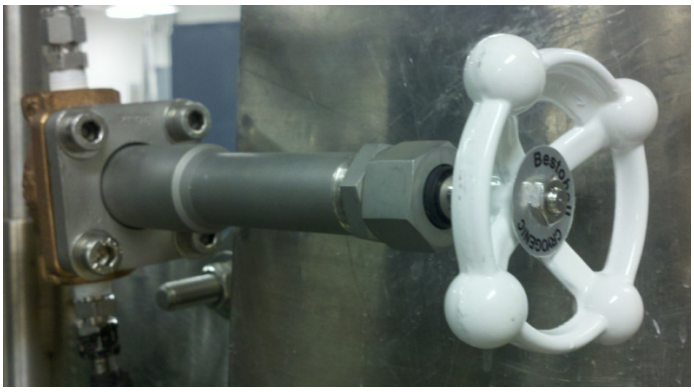

Figure 9. Cryogenic globe valve.

3.2 Experimental Design and Setup

This section goes over the design of the components in the experiment as well as their function in the system.

3.2.1 Rig Design

The high heat transfer test rig consists of a solid copper block, copper test section, 1/8” (0.32 cm) outside diameter copper channel with 0.014” (0.04 cm) wall thickness, aluminum test section cradle, and a stainless steel frame. The copper block has a tapered end and a flat end. The tapered end narrows to a flat face with the area the size of the test section, 2” x 1” (5.1 cm x 2.5 cm). The 4” x 4” (10 cm x 10 cm) flat end has 25 drilled shafts designed to slide in the heating cartridges which will heat the block to the desired temperature. Only 21 of the 25 drilled shafts were used for the experiments conducted in this thesis. The total length of the copper block is 7” (18 cm). The material, copper, was chosen for its high thermal conductivity allowing for high heat conduction to the test section and channel. The tapered end of the copper block allows for the heat conduction to geometrically focus on a concentrated area the size of the test section. Based on computational analysis done by the Air Force Research Laboratory Propulsion Directorate using the commercial software CFD++, the heat transfer of the block to the test

section is greatest when using a rectangular prismatic block with a tapered end opposed to a cylindrical solid with or without a tapered end [6],[7]. The assembly of the experiment inside the vacuum chamber can be seen in Figure 10.

Figure 10. Assembled heating block.

The copper test section holds the channel in place. The aluminum cradle is placed above the test section to keep it secure to insure the test section is touching the heating block. The test section cradle is bolted on to the top of the steel frame securely locking the test section and cradle in place. The white plates noticeable in Figure 10 are 1/16” (0.16 cm) ceramic plates in placed between the aluminum cradle and the copper heating block to make sure the heat conduction from the heating block is going straight to the copper test section. Also, the aluminum cradle is not compromised by the high temperatures approaching the melting point of alumnium. The ceramic used is a machineable glass ceramic which can remain stable in temperatures up to 1000 °C (1832 °F).

In the experiment 21 heating cartridges were wired to five relays. Each relay in the experiment was linked to its own thermocouple to control the temperature in the heating cartridges on the corresponding relay. Only the channel temperatures were recorded on the DAQ while the block temperatures were only used for controlling the heating cartridges on the relays using the temperature controller. The heating block and the components touching the block were all placed inside a vacuum chamber while the solid state relays, temperature controller, DAQs, and majority of the piping were placed outside the vacuum chamber.

In order to get a temperature profile of the cooling channel, six equally spaced thermocouples were placed on top of the test section measuring the channel temperature opposite the side of the heating source as seen in Figure 10. Each K-type thermocouple along the channel has a threaded end allowing each thermocouple to be screwed in the threaded holes on the test section. Having the thermocouples screw in place allows for contact between the thermocouple bead and the channel. The continuity of the thermocouples to the channel was checked with a voltmeter to guarantee contact. The temperature controller thermocouples were placed on the heating block with a high temperature ceramic adhesive called Resbond™ 919 Electrically Resistant. The ceramic adhesive secured the thermocouples on the surface of the heating block. The Resbond™ was also placed at the exit of the heating cartridges to prevent the cartridge cables from receiving the same temperatures of the heating block preventing them from burning out.

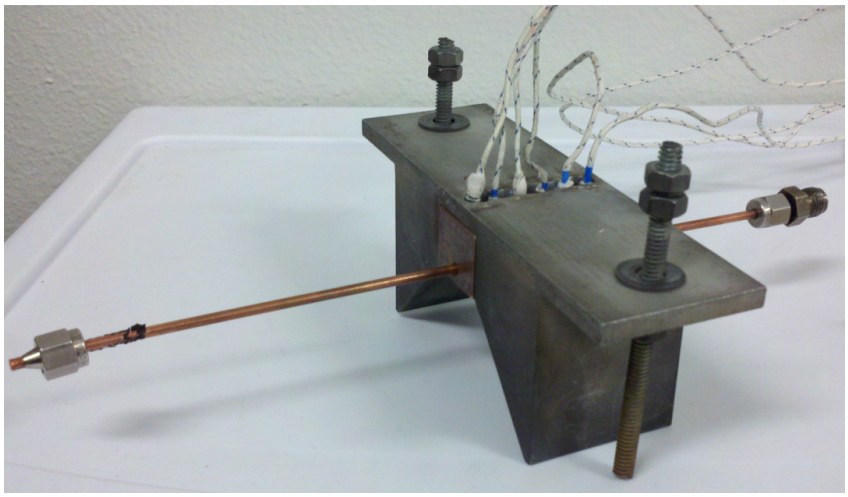

Figure 11. Assembled cooling channel with thermocouples.

The liquid nitrogen and liquid methane were designed to enter the copper channel through an insulated stainless steel line with Swagelok connections. A schematic of the piping can be seen in the appendix. The pressure transducers before and after the channel shown in the schematic are used to provide an estimate of the fluid pressure and fluid flow rate using the pressure difference from exit and inlet of the channel. The experiment was designed so the liquid can have a steady state flow through the channel. The six thermocouples on the channel record the temperatures during the experiment onto the DAQ. All the data gathered by the thermocouple DAQ and pressure transducer DAQ were compiled using a LabVIEW program.

The exiting methane goes an empty 50 L gas cylinder for use as a catch tank to hold the exiting methane. Once the methane is in the cylinder in gaseous form it can be burned off to re-empty the tank

3.2.2 Flow Rate

The flow rate in the experiment was intended to closely resemble the fuel flow rate of a 1 (4.45 N) to 10 lb (44.5 N) thrust rocket engine with a given specific impulse (I_{sp}) of 320 s as seen

in Table 1. The thrust and specific impulse used for this experiment were chosen by using the preliminary specifications set in the design of the cSETR rocket. The flow rates were determined using the formula that relates specific impulse and thrust, equation (1).

$$F = I_{sp}\,\dot{\omega}_p \qquad (1), [2]$$

In the equation F is thrust and $\dot{\omega}_p$ is the total weight flow rate including fuel and oxidizer. The flow rates for both oxidizer and fuel can be found using the mixture ratio (MR) which compares oxidizer flow rate by weight, ω_o, and fuel flow rate by weight, ω_f, equation (2).

$$MR = \frac{\omega_o}{\omega_f} \qquad (2), [2]$$

Table 1. Fuel flow rate determined from designed thrust in a rocket engine.

Thrust (lb)	Thrust (N)	Mixture Ratio	Total Weight Flow Rate (N/s)	Total Mass Flow Rate (kg/s)	Fuel Flow Rate (kg/s)	Oxidize Flow Rate (kg/s)	Isp (s)
1.00	4.45	3.20	1.39E-02	1.42E-03	3.37E-04	1.08E-03	320
2.00	8.90	3.20	2.78E-02	2.83E-03	6.75E-04	2.16E-03	
3.00	13.3	3.20	4.17E-02	4.25E-03	1.01E-03	3.24E-03	
5.00	22.2	3.20	6.95E-02	7.08E-03	1.69E-03	5.40E-03	
7.00	31.1	3.20	9.73E-02	9.92E-03	2.36E-03	7.56E-03	
10.0	44.5	3.20	1.39E-01	1.42E-02	3.37E-03	1.08E-02	

Chapter 4

RESULTS

Tests were run on the heat transfer rig with LN_2 rig before starting any LCH_4 tests.

4.1 Radiation and Heat Flux

In a vacuum heat loss due to convection is assumed to be negligible; however, the heating block is not immune to the heat loss due to radiation. In order to estimate the radiation loss a radiometer with a viewing angle of 150º was placed inside the vacuum chamber 4" (10.2 cm) away from the surface of the heating block at different heat flux conditions. Each heat flux condition has a different amount of power going into the heating block which is adjusted by the number of solid state relays turned on. The power output from each relay was found using the heating cartridge power output specified by the manufacturer, Omega.

The experiment was run at five different heat fluxes keeping a constant heat flux starting at 891 kW/m^2 (0.545 Btu/s-in^2) and ending in 3743 kW/m^2 (2.29 Btu/s-in^2). Table 2 shows the amount of heating cartridges placed in each relay along with the power output for each relay. Each relay corresponds to a different heat flux condition. The theoretical radiation heat loss was calculated assuming thermal radiation between parallel plates and then compared with data taken from the radiometer. The heat transfer due to radiation between the copper heating block and the radiometer was found using equation (3) where σ is the Stefan-Boltzmann constant, T_1 is the heating block temperature, T_2 is the radiometer temperature, ε_1 is the emissivity of the copper block, and ε_2 is the emissivity of the radiometer. For the assumption of thermal radiation

between parallel plates A_1 and A_2 are of equal area equivalent to the area of one face of the heating block, 7" by 4".

$$\dot{Q}_{12} = \frac{\sigma(T_1^4 - T_2^4)}{\frac{1-\varepsilon_1}{A_1\varepsilon_1} + \frac{1}{A_1F_{12}} + \frac{1-\varepsilon_2}{A_2\varepsilon_2}} \qquad (3), [8]$$

The heat flux obtained from the radiometer in Table 3 is for one side of the block which is multiplied by four to obtain the estimated total heat flux loss due to radiation throughout the entire block. When comparing theoretical and measured radiation heat flux, radiometer readings appear to be lower with a percent error between the two of approximately 15% to 30% seen in Table 4. The theoretical power loss was calculated to be between 1% to 2.5% as seen in Table 2.

Table 2. Heat Rig Radiation Loss

Relay number	1	2	3	4	5
Cartridges (1 = 400W [0.38 Btu/s-in^2] & 178 kW/m^2 [0.109 Btu/s-in^2])	5	9	13	17	21
Heat Flux (kW/m^2) [Btu/s-in^2]	891 [0.545]	1604 [0.981]	2317 [1.42]	3030 [1.85]	3743 [2.29]
Power Output (W) [Btu/s]	2000 [1.90]	3600 [3.41]	5200 [4.89]	6800 [6.45]	8400 [7.96]
Block Temperature (°C) [°F]	150 [302]	200 [392]	315 [599]	350 [662]	400 [752]
Percent Power Loss Due to Radiation (%)	1.08	1.12	2.26	2.23	2.52

Table 3. Heat flux using radiometer

Relay Number	1	2	3	4
Cartridges	5	9	13	17
Temperature Reached, T_1 (°C) [°F]	150 [302]	200 [392]	315 [599]	350 [662]
Heat Flux (kW/m^2) [Btu/s-in^2]	0.23 [1.43E-4]	0.37 [2.29E-4]	1.31 [8.04E-4]	1.65 [1.01E-3]

Table 4. Calculated and Experimental Heat Flux Loss

Temp (°C)[°F]	Experimental Loss (kW/m^2) [$Btu/s\text{-}in^2$]	Calculated Loss (kW/m^2) [$Btu/s\text{-}in^2$]	Percent Error (%)
150 [302]	0.234 [1.43E-4]	0.279 [1.71E-4]	16
200 [392]	0.374 [2.29E-4]	0.52 [3.18E-4]	28
315 [599]	1.314 [8.04E-4]	1.52 [9.27E-4]	13
350 [662]	1.648 [1.01E-3]	1.96[1.2E-3]	16

4.2 Liquid Nitrogen Test Results and Analysis

Each experiment using LN_2 was conducted in the same manner with primary steps of pulling vacuum in the system, heating the block to the desired temperature and constant heat flux, and flowing liquid nitrogen. During the flow of LN_2 data was recorded for about 8 to 10 minutes to obtain steady state flow. The thermocouples on the channel were all checked for continuity between the thermocouple and channel to insure they were in direct contact with the outer wall of the channel. Four tests were run for the first heat flux, three tests for the second heat flux, and two tests were run for the remaining heat flux conditions all showing a similar pattern. The first three thermocouples TC1, TC2, and TC3 shared a decreasing trend in temperature in all four tests of the first heat flux condition while temperatures further along the channel TC4, TC5, and TC6 recorded an increasing trend in temperature. Figure 12 is an example at the first heat flux condition along the length of the channel at different times. The tests were run with an LN_2 tank pressure of about 0.827 MPa (120 psi). All the thermocouples before running any liquid were recording values at the same starting temperature each corresponding to temperature at the heat flux level. The third, fourth, and fifth heat flux conditions were run under slightly higher LN_2 tank pressure, 150 psi (1.03 MPa). The data of the five different heat flux tests can be found in the appendix. Each plot shows distributions at 100 s,

200 s, 300 s, 400 s, and 500 s for each test as well as the normalized plots for each, in the form of Figure 13. The majority of the test data result in a similar behavior as in Figure 12 where liquid appears to flow at the beginning of the channel while at the end of the channel the recorded temperatures are higher where a possible boil off occurs.

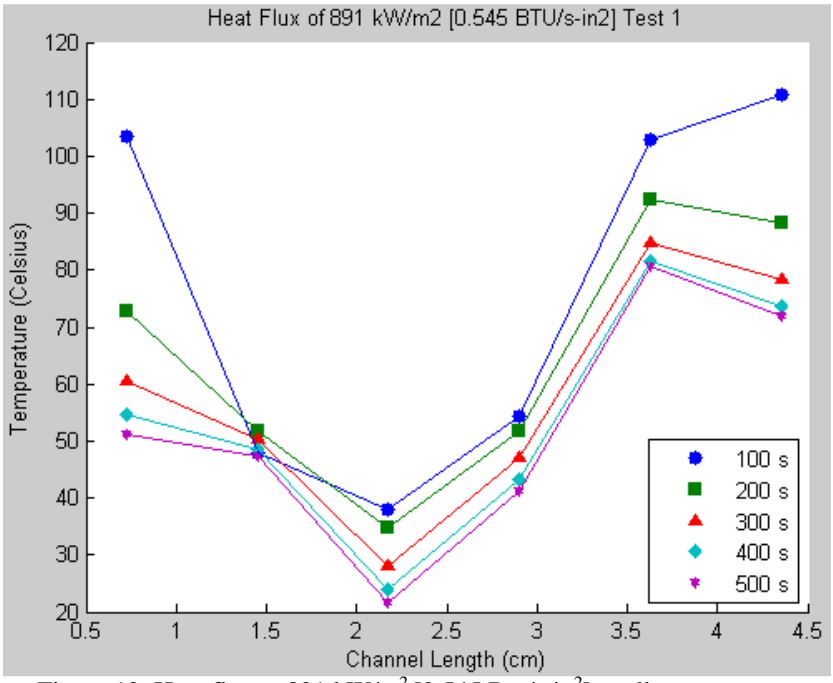

Figure 12. Heat flux at 891 kW/m^2 [0.545 Btu/s-in^2], wall temperature.

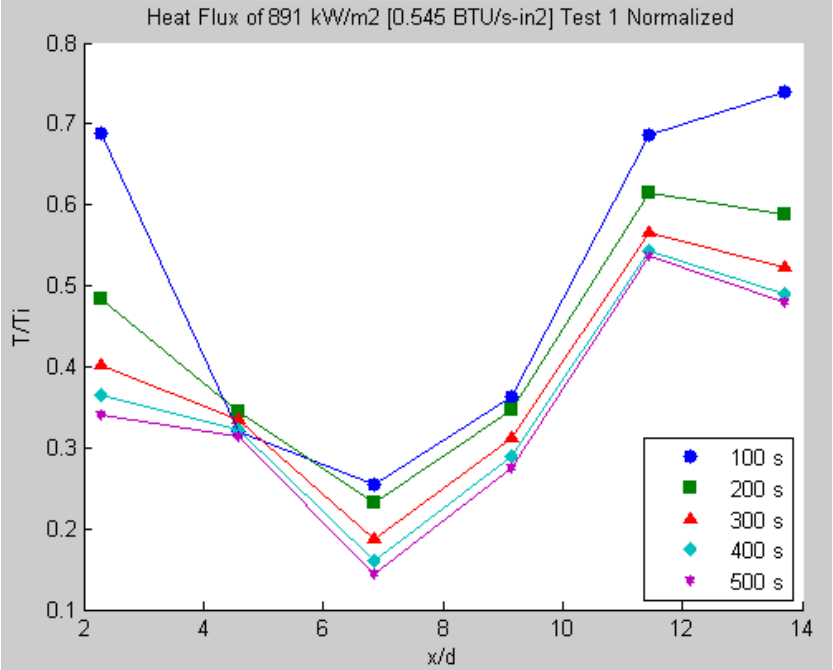

Figure 13. Heat flux at 891 kW/m^2 [0.545 Btu/s-in^2] normalized plot

Since the temperature of the channel is well above the boiling point of LN_2 boil off is likely taking place inside the channel. A combination of nucleate boiling and film boiling is occurring inside the channel. Knowing of the possible boil off, it can be speculated that towards the exit of the channel the LN_2 flowing through has formed a layer of vapor along the heated wall surface causing vapor lock. The vapor layer is separating the liquid from the heated channel wall as seen in Figure 14 resulting in higher temperature readings at the exiting thermocouples since liquid is not in direct contact with the channel wall. When the LN_2 left the experiment after it flowed through the channel, there was condensation on the surface of the piping while liquid was also being captured in the exiting catch dewar; this showed that the LN_2 did not completely vaporize and was exiting the channel in liquid form.

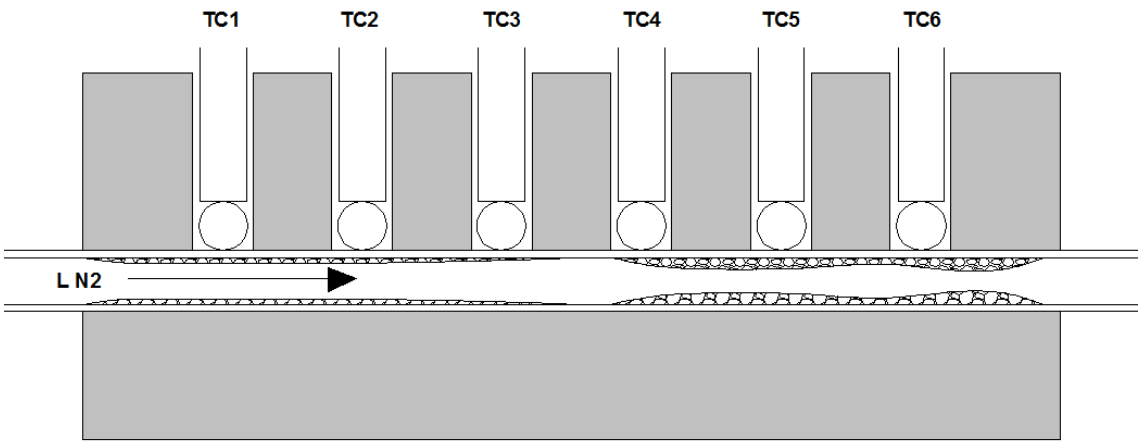

Figure 14. Channel with vapor on the channel wall at TC4, TC5, and TC6

When looking at an equation for heat transfer in a pipe with constant heat flux coming from one direction equation (2) can be derived where T_m is the mean temperature, T_i is the inlet temperature, q_s is the heat flux, P is the perimeter of the pipe, $\dot{m}$ is the mass flow rate, and x is the distance along the pipe.

$$T_m = \frac{q_s P}{\dot{m} C_p} x + T_i \qquad (4), [14]$$

As the heat flux increases in the equation the slope of the line increases when plotting temperature with distance. When keeping a constant heat flux the only changing variable, assuming steady state flow and constant mass flow rate, will be the initial temperature. In the different tests done in the experiments with constant heat flux similar patterns can be found when plotting temperature with distance. With constant heat flux being applied to the channel the temperature in the channel is expected to increase uniformly.

At the third heat flux condition a new L N_2 tank was used with different tank pressures as seen in Table 5 causing different estimated flow rates than previous tests, the data follows the same pattern. The estimated flow rate was gathered using an average wall temperature, inlet pressure, and pressure difference along the channel. A density could be found from NIST tables

[9] using the temperature and pressure to estimate a quality of LN_2 inside the channel. Since the temperature used for determining the density was the channel exterior wall temperature and not the fluid temperature the flow rates on Table 5 can only be used as a reference to each other for noticing difference in flow rate in the beginning experiments and the ending experiments.

Table 5. Inlet Pressure and Estimated Flow Rate													
Heat Flux (kW/m^2) [$BTU/s\text{-}in^2$]	Heat Flux 1 891 [0.545]				Heat Flux 2 1604 [0.981]			Heat Flux 3 2317 [1.42]		Heat Flux 4 3030 [1.85]		Heat Flux 5 3743 [2.29]	
Test Number	1	2	3	4	5	6	7	8	9	10	11	12	13
Approximate LN_2 Pressure (psi) [MPa]	140 [0.97]	140 [0.97]	120 [0.83]	120 [0.83]	120 [0.83]	120 [0.83]	120 [0.83]	100 [0.69]	170 [1.2]	100 [0.69]	90 [0.62]	110 [0.76]	90 [0.62]
Estimated Flow Rate (lbm/s) [g/s]	1.0E-3 [0.45]	8.7E-4 [0.39]	8.8E-4 [0.40]	8.5E-4 [0.38]	8.0E-4 [0.36]	7.6E-4 [0.35]	7.4E-4 [0.34]	4.1E-4 [0.19]	8.7E-4 [0.39]	4.1E-4 [0.19]	4.1E-4 [0.19]	3.3E-4 [0.15]	3.3E-4 [0.15]

In the higher heat fluxes starting from the third heat flux condition, the trend tends to start sooner with a rise in temperature in the third thermocouple as seen in the higher heat flux figures in the Appendix. However, the vapor lock effect still seems to be present in all cases. As the heat flux increases for the different conditions so does the coolant side wall temperature as would be expected as seen in Figure 15.

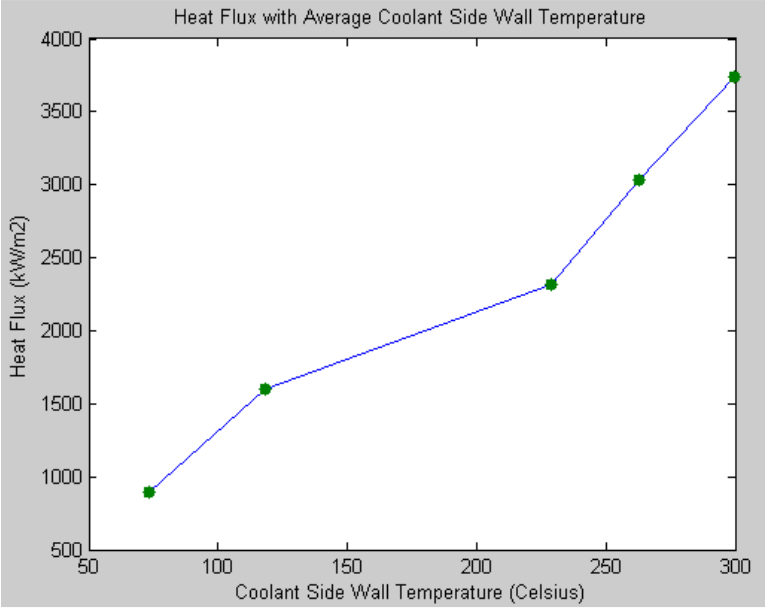

Figure 15. Average coolant side wall temperature compared to heat flux.

4.3 Liquid Methane Test Results and Analysis

Preliminary LCH_4 tests were run on the system to validate the system's ability to handle the fuel it was designed for. While a 180 L tank was available for running LN_2 tests, the lack of LCH_4 available in the area required LCH_4 to be produced in the lab. Using a 1 L, insulated heat exchanger designed by cSETR, LCH_4 was condensed in a dewar pressurized by gaseous methane. The dewar has an 1/8" (0.32 cm) diameter piping coiled inside which allows for the flow of LN_2. When the gaseous methane touches the surface of the LN_2 coil, the cryogenic temperature causes the gas to condense. A scale was placed under the dewar as seen in Figure 16 to measure the amount of LCH_4 produced using an approximate density of the liquid with the temperature gathered by the E-Type thermocouple in the dewar. When running an experiment with LCH_4, vacuum was pulled in the entire system while the heating block was set to the desired heat flux. The storage tanks were then chilled with LN_2 for about 5 to 10 minutes. The production of LCH_4 began once the heating block approached the temperature designated by the heat flux condition. Once the LCH_4 was made the tanks were chilled again and vacuum pumped

while the production dewar was prepared for transferring LCH_4. Transferring LCH_4 consisted of carefully flipping the dewar upside down to attach to the run tanks. The valves connecting the dewar and tanks were then opened allowing the LCH_4 to transfer from the dewar to the chilled run tanks.

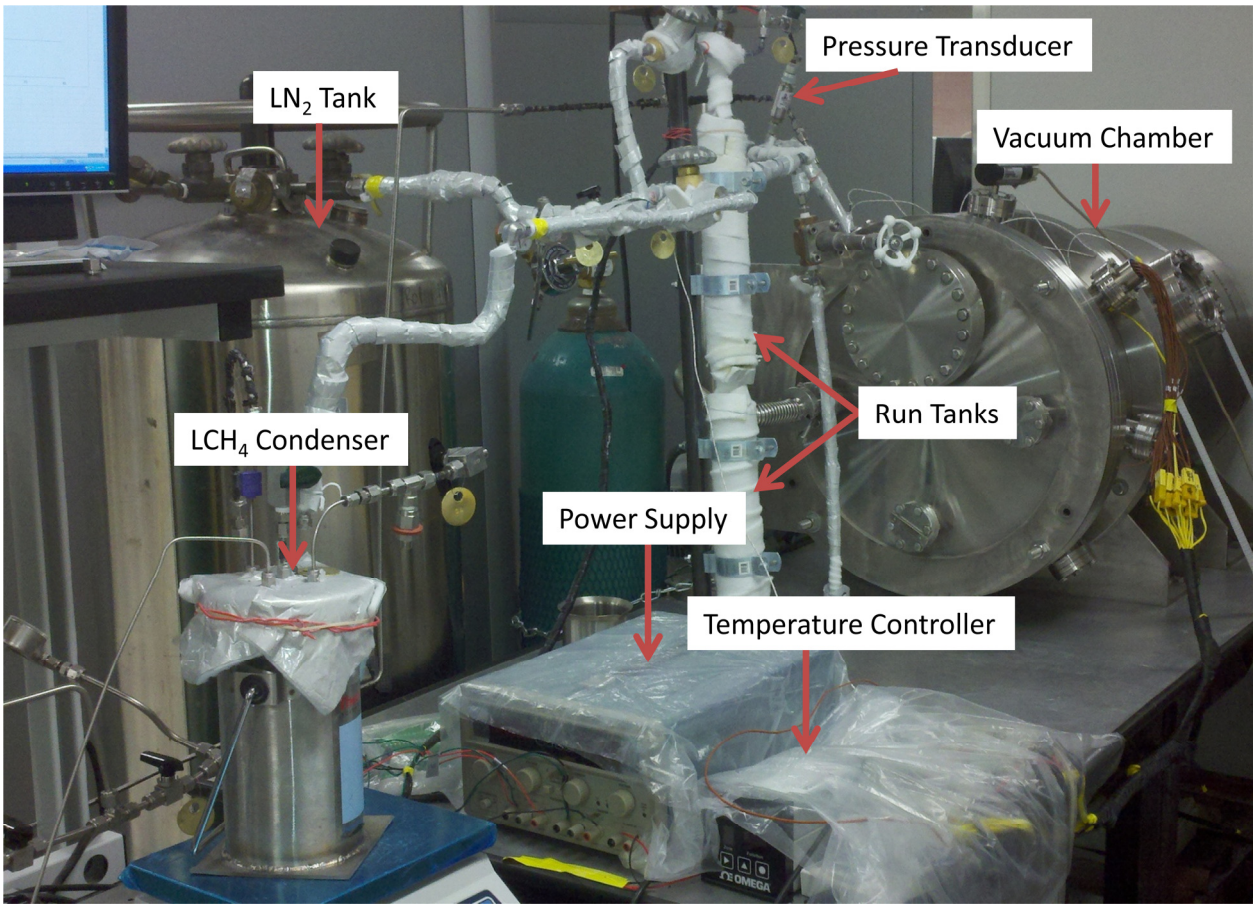

Figure 16. Entire heat rig system setup for testing

The LCH_4 tests were run under less time than the LN2 tests since less liquid was available for use in testing. These tests were also run using helium at 100 psi (0.69 MPa) to push out the LCH_4 from the tanks. Figures 17 and 18 are temperature profiles with distance for the two LCH_4 experiments were run. In the first test the temperature profile along the channel increases with distance along the channel and with time. In the second test the first and last thermocouples

show lower temperatures than TC2 through TC5. While the same vapor lock phenomena can be present in these tests like the in LN_2 tests, it is best to run the experiments with more LCH_4 available to achieve a steady state flow and repeatability for comparisson with the LN_2 tests, considering there was boil off of LCH4 during the transfer.

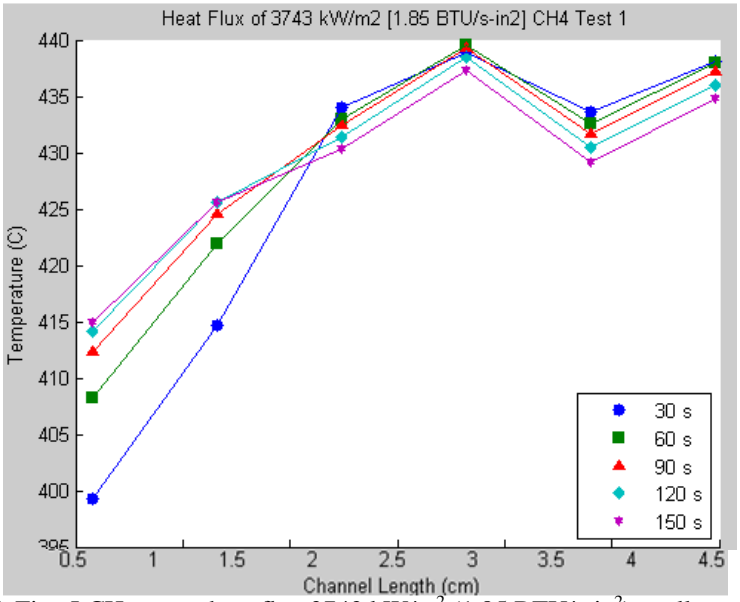

Figure 17. First LCH_4 test at heat flux 3743 kW/m^2 (1.85 BTU/s-in^2), wall temperature.

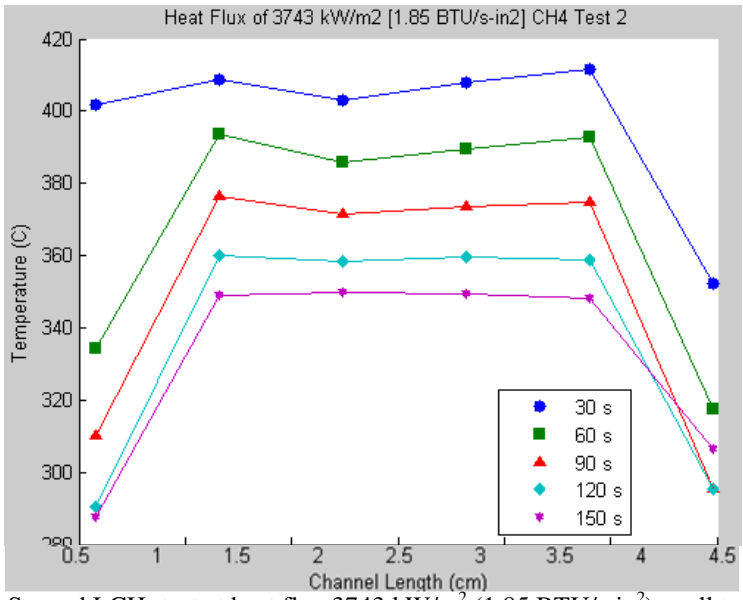

Figure 18. Second LCH_4 test at heat flux 3743 kW/m^2 (1.85 BTU/s-in^2), wall temperature.

Chapter 5

CONCLUSIONS

5.1 Conclusions

The cSETR heat transfer rig was able to produce repeatable results during the heat tests and LN_2 tests. With preliminary tests done on the rig it is possible to continue experimentation using LCH_4. In the rig the radiation heat losses are minimal and the testing in vacuum discards the convectional heat losses in the system; therefore, the channel receives its increase in temperature directly through conduction from the heating block. The channel will then be able to reach the temperatures of the heating cartridges given enough time for conduction to reach the channel. The LN_2 data suggests something is keeping the thermocouples from reading the temperatures of the fluid in some locations along the channel. The difference in temperature from the LN_2 and the channel wall, which is significantly above the boiling point of LN_2, leads to boil off. The boil off of LN_2 is believed to remain in the channel as a vapor layer along the wall leading to the existence of vapor lock in the channel. The LCH_4 tests do not provide enough consistency with just under a liter of liquid for each test. A tank with a greater volume will be needed to produce more methane for experiments comparable to those of LN_2.

5.2 Recommendations and Future Work

The liquid methane storage tank held a volume of 1 L, but to better achieve a steady state flow of liquid methane through the channel a larger amount of liquid methane is needed. In addition, the current process of transferring liquid methane to the storage tank triggers some loss of liquid due to boil off in the transfer. The production tank's pressure limitation did not allow

for the experiment to run from that tank; this can be resolved with future alterations to the experiment. Flow meters and in line thermocouples will be added to the system for finding liquid flow rates and determining the quality of fluid in and out of the channel. If the channel thermocouples were welded on to the channel there would be question whether contact is lost during experimentation with the vibrations of the channel with high pressures.

In the experiment the cross sectional shape of the channel was kept constant, circular, during testing; in future experiments the shape and size of the channel cross section can be changed. Triangular and square channels with varying aspect ratios might provide results that are worth investigating for use in cooling channels. Also, using other fluids used in rockets such as kerosene and liquid oxygen can provide more insight into the use of different rocket fuels for cooling in a rocket regenerative cooling system. The test section and channel material can also be changed to incorporate metal alloys typically found in rockets. This experiment was conducted with temperatures up to 400 °C (752 °F); the cSETR expects to explore temperatures greater than 650 °C; to reach these temperatures the heating cartridges need to withstand the high temperatures avoiding blow out.

REFERENCES

[1] Huzel, D.K., Huang, D.H., Modern Engineering for Design of Liquid-Propellant Rocket Engines. Washington DC: AIAA 1992.

[2] Brown, C.D., Spacecraft Propulsion. Washington DC: AIAA 1996.

[3] Billingsley, M.C., Lyu, H.Y., Bates, R.W., "Experimental and Numerical Investigations of RP-2 Under High Heat Fluxes", Air Force Research Laboratory, Propulsion Directorate, Edwards AFB, CA, May 2007.

[4] Schuff, R., Maier, M., Sindiy, O., Ulrich, C., Fugger, S., "Integrated Modeling and Analysis for LOX/Methane Expander Cycle Engine: Focusing on Regenerative Cooling Jacket Design", AIAA, Joint Propulsion Conference & Exhibit, Sacramento, CA, July 2006.

[5] Burkhardt, H., Sippel, M., Herbertz, A., Klevanski, J., "Comparative Study of Kerosene and Methane Propellant Engines for Reusable Liquid Booster Stages", 4th International Conference on Launcher Technology, Space Launcher Liquid Propulsion, Koln, Germany, December 2002.

[6] Maas, E., Irvine, S., Bates, R., Auyeung, T., "A High Heat Flux Facility Design for Testing of Advanced Hydrocarbon Fuel Thermal Stability", Air Force Research Laboratory Propulsion Directorate, Edwards AFB, CA, December 2004.

[7] Bates, R.W., Maas, E.D., Irvine, S.A., Auyeung, T.P., "Design of a High Heat Flux Facility for Thermal Stability Testing of Advanced Hydrocarbon Fuels", Air Force Research Laboratory Propulsion Directorate, Edwards AFB, CA, April 2004.

[8] Cengel, Yunus, and Ghajar Afshin. Heat and Mass Transfer. 4th ed. McGraw-Hill, 2010. 737.

[9] "Thermophysical Properties of Nitrogen" in NIST Chemistry WebBook, NIST Standard Reference Database Number 69, National Institute of Standards and Technology (NIST), Gaithersburg MD, 208992011, http://webbook.nist.gov/cgi/cbook.cgi?ID=C7727379&Mask=4 (Retrieved August 16, 2011).

APPENDIX

Appendix A: Rig Development

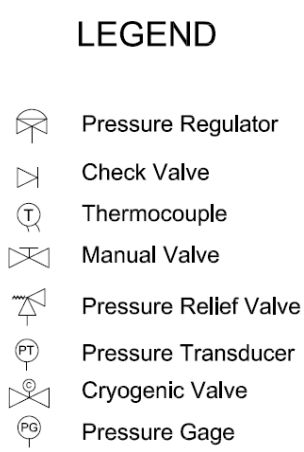

Figure 19. Legend of schematic piping.

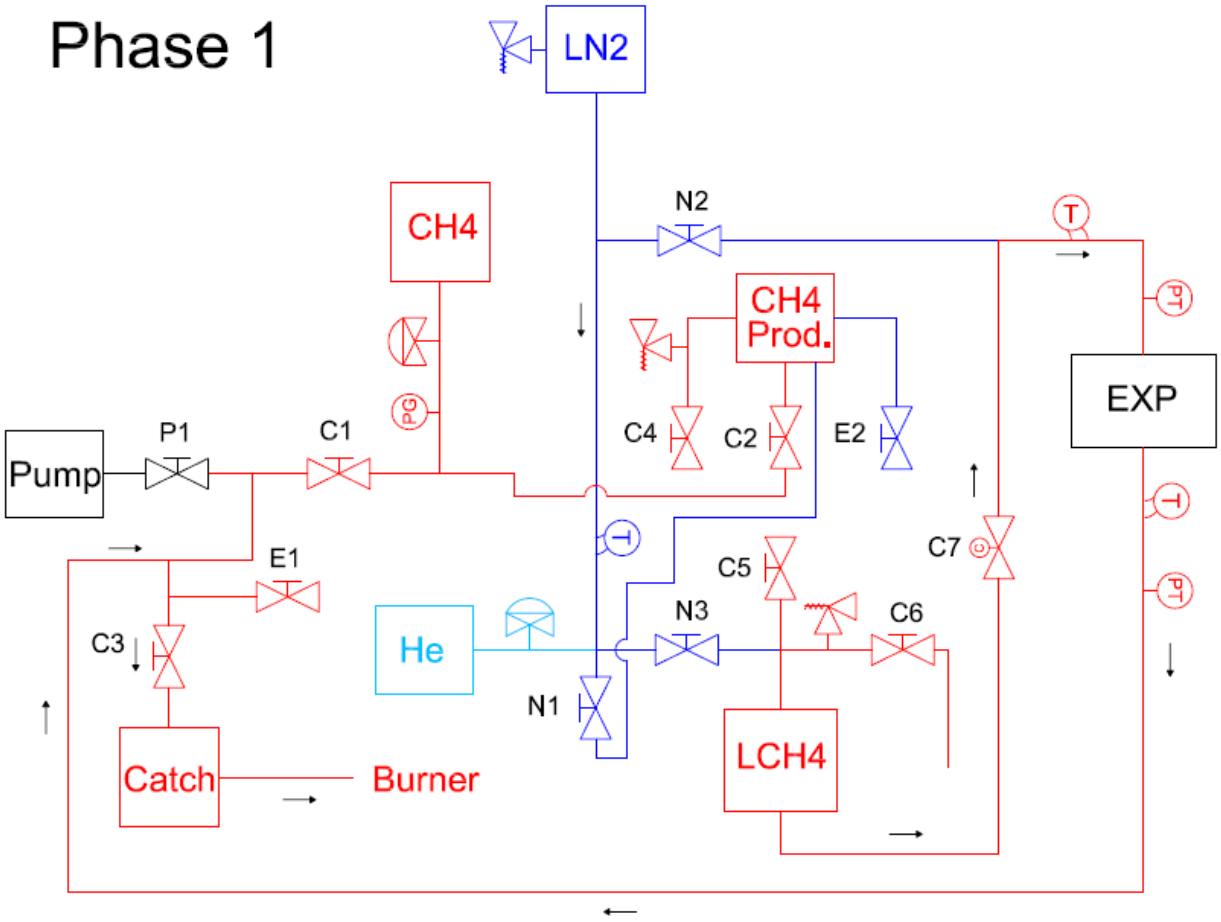

Figure 20. Phase 1 of schematic with methane production.

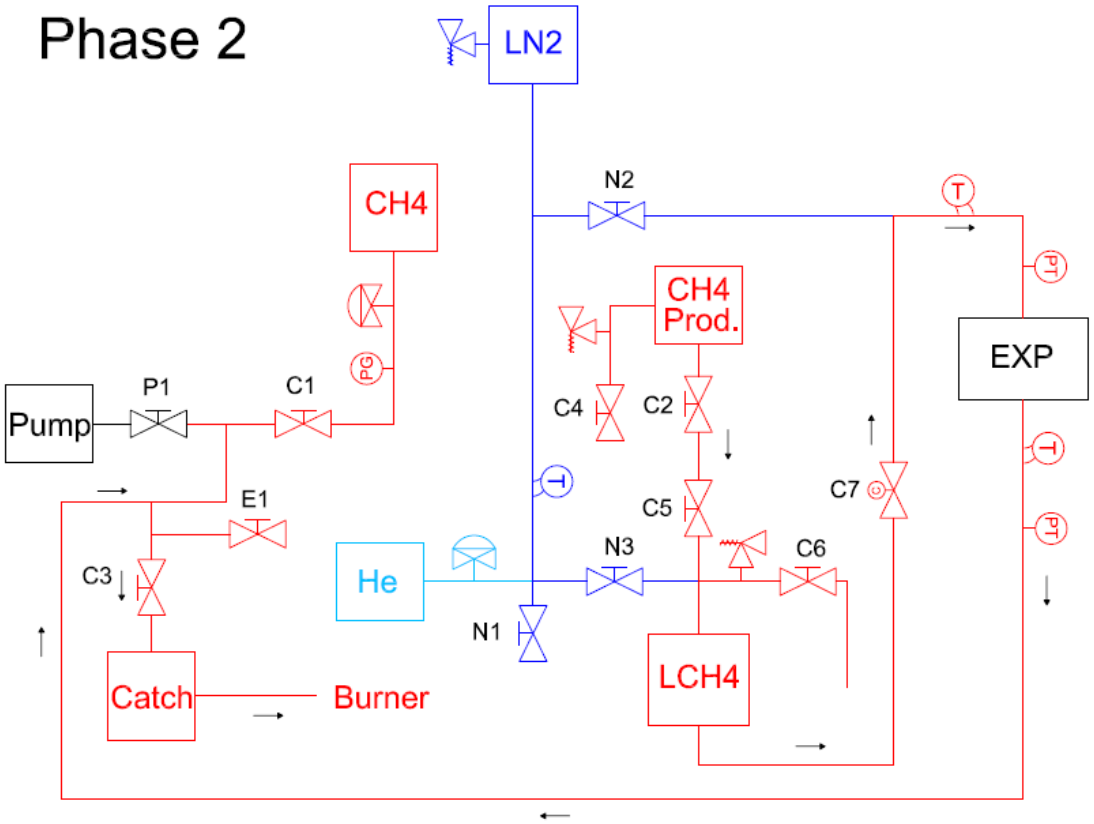

Figure 21. Phase 2 of schematic with run tank.

Appendix C: Channel Wall Temperature with Distance Plots

(+/-) Error (°C)					
TC1	TC2	TC3	TC4	TC5	TC6
0.8	0.9	1	0.8	0.7	0.7

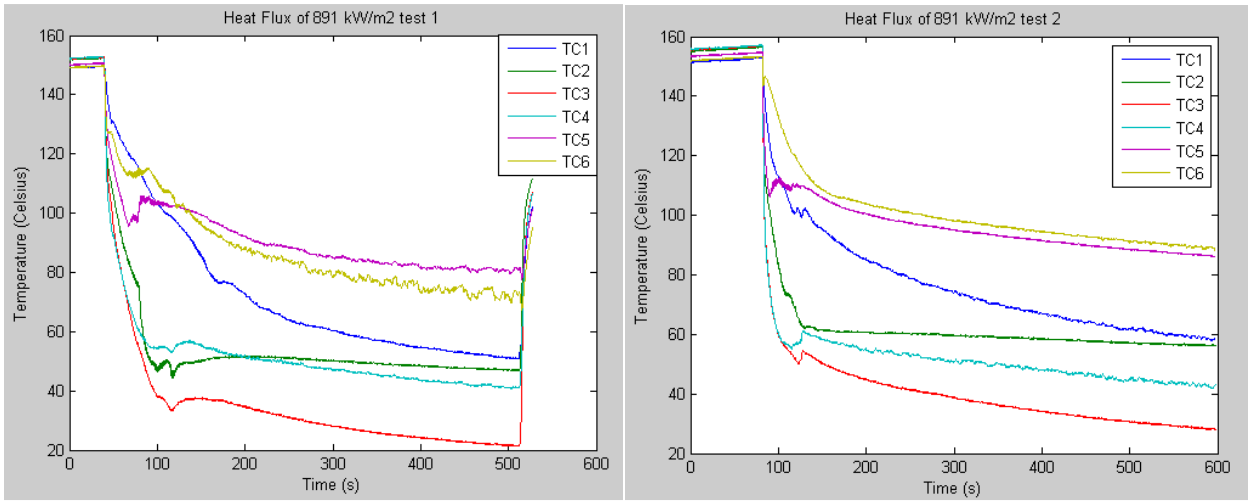

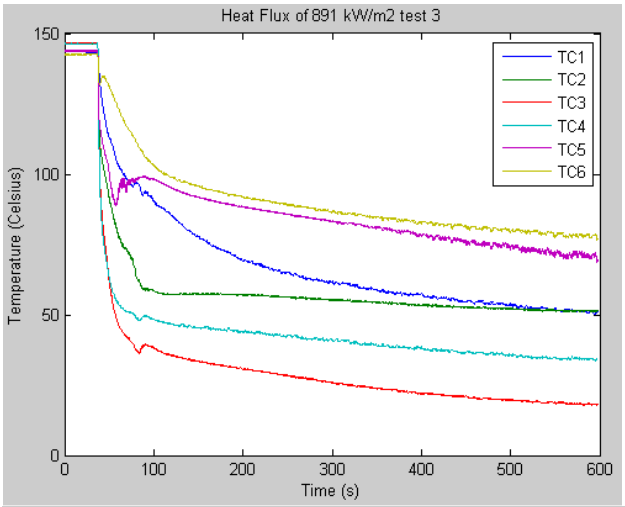
Heat Flux of 891 kW/m2 test 3
Temperature (Celsius)
Time (s)
TC1
TC2
TC3
TC4
TC5
TC6

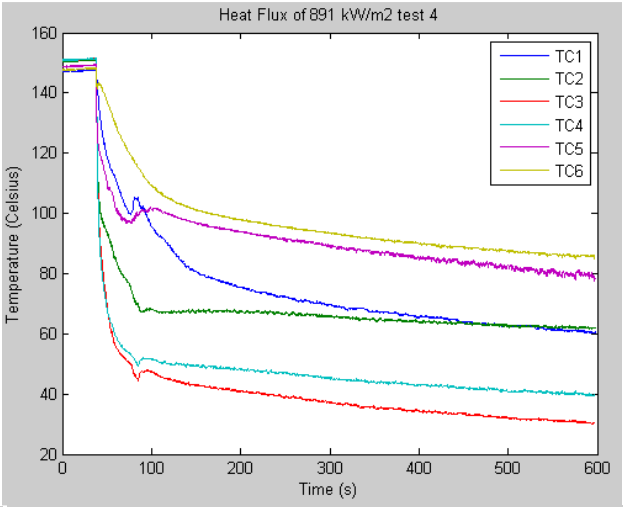
Heat Flux of 891 kW/m2 test 4
Temperature (Celsius)
Time (s)
TC1
TC2
TC3
TC4
TC5
TC6

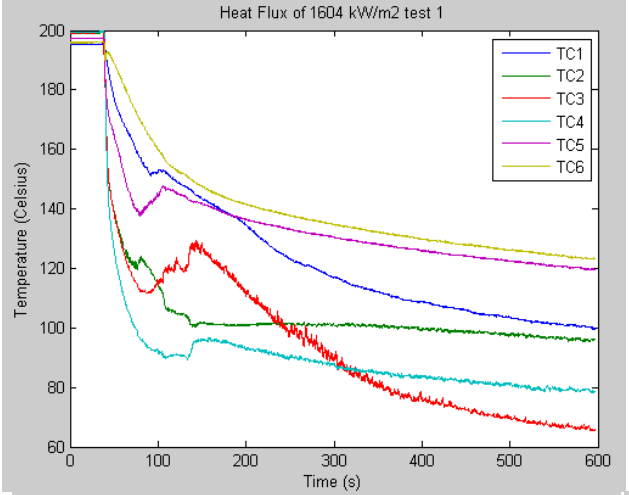
Heat Flux of 1604 kW/m2 test 1
Temperature (Celsius)
Time (s)
TC1
TC2
TC3
TC4
TC5
TC6

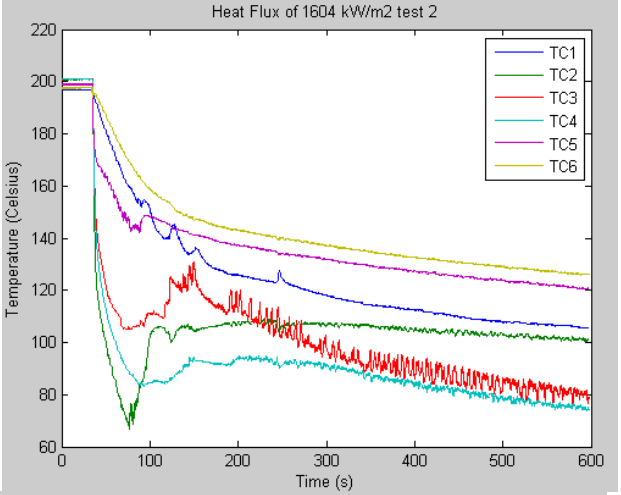
Heat Flux of 1604 kW/m2 test 2
Temperature (Celsius)
Time (s)
TC1
TC2
TC3
TC4
TC5
TC6

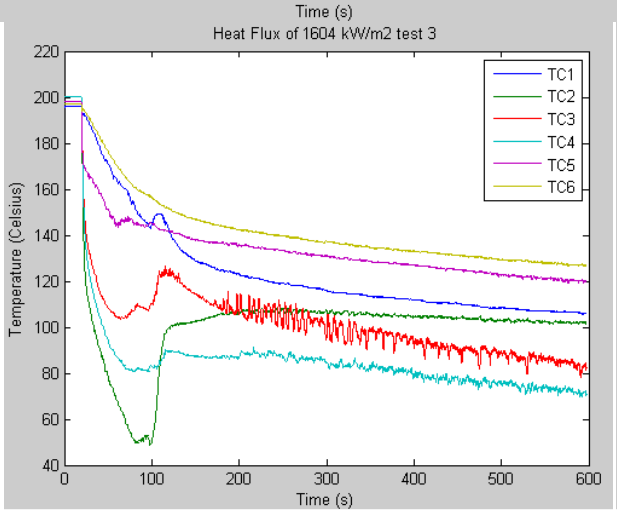
Heat Flux of 1604 kW/m2 test 3
Temperature (Celsius)
Time (s)
TC1
TC2
TC3
TC4
TC5
TC6

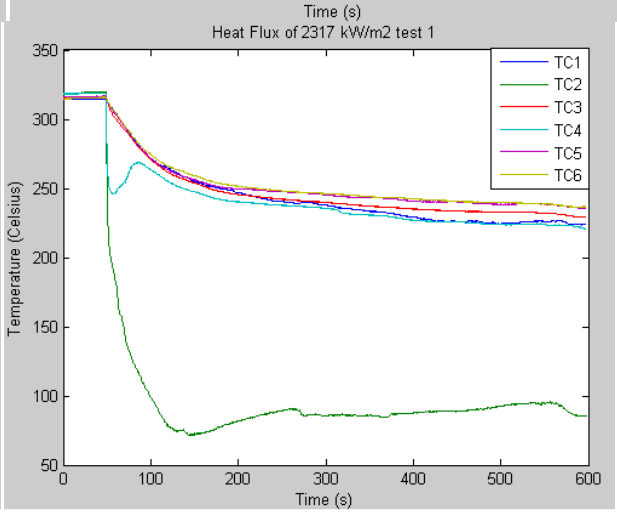
Heat Flux of 2317 kW/m2 test 1
Temperature (Celsius)
Time (s)
TC1
TC2
TC3
TC4
TC5
TC6

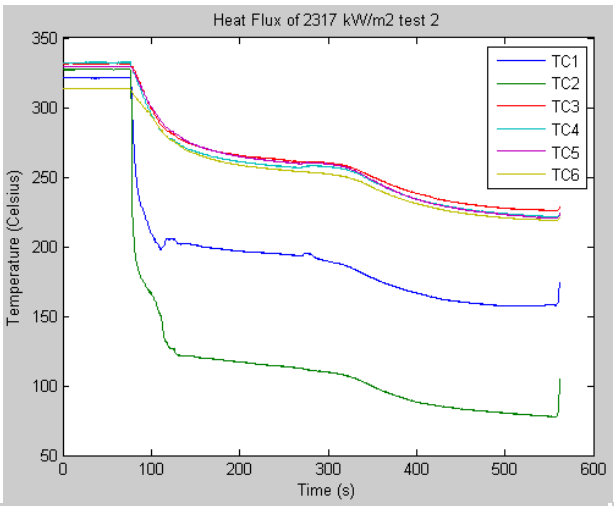
Heat Flux of 2317 kW/m2 test 2
Temperature (Celsius)
Time (s)
TC1
TC2
TC3
TC4
TC5
TC6

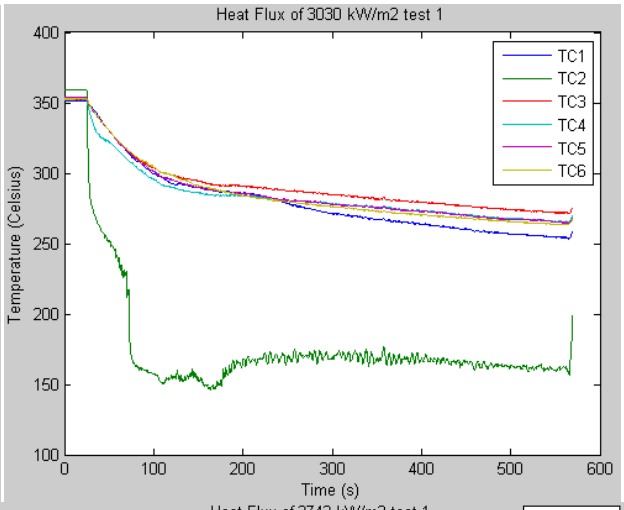
Heat Flux of 3030 kW/m2 test 1
Temperature (Celsius)
Time (s)
TC1
TC2
TC3
TC4
TC5
TC6

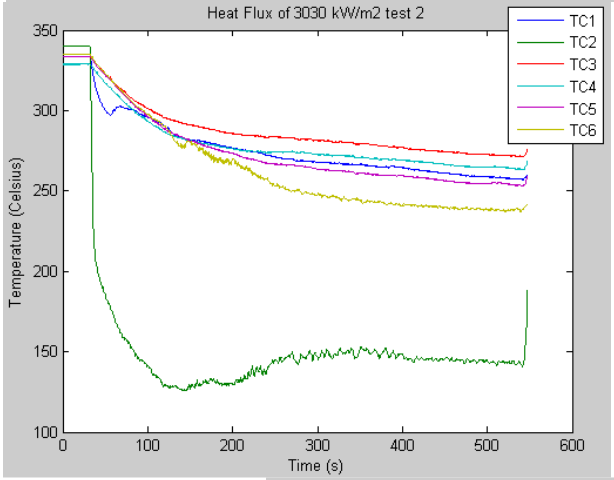
Heat Flux of 3030 kW/m2 test 2
Temperature (Celsius)
Time (s)
TC1
TC2
TC3
TC4
TC5
TC6

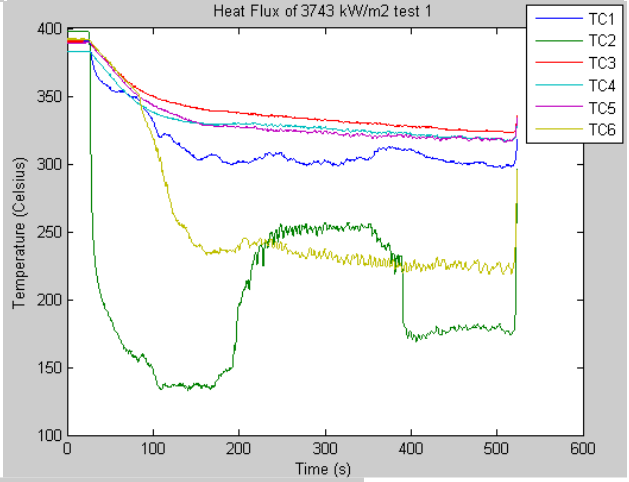
Heat Flux of 3743 kW/m2 test 1
Temperature (Celsius)
Time (s)
TC1
TC2
TC3
TC4
TC5
TC6

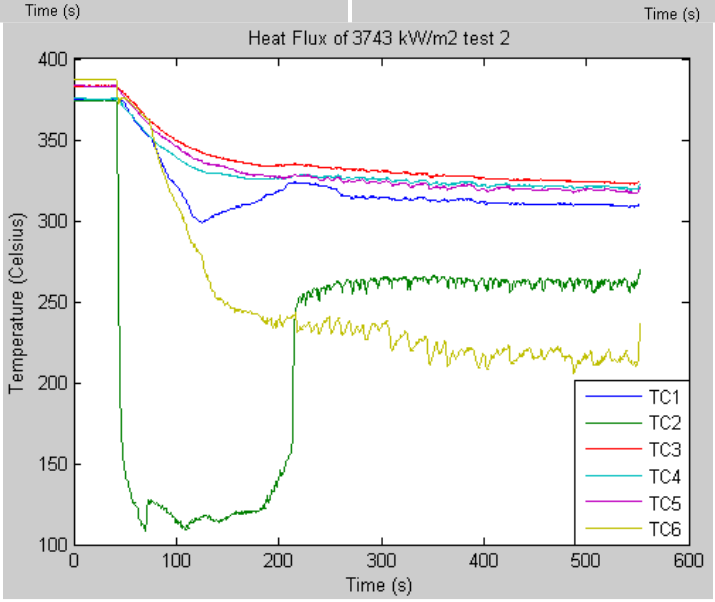
Heat Flux of 3743 kW/m2 test 2
Temperature (Celsius)
Time (s)
TC1
TC2
TC3
TC4
TC5
TC6

Appendix C: Channel Wall Temperature with Distance Plots

(+/-) Error (°C)					
TC1	TC2	TC3	TC4	TC5	TC6
0.8	0.9	1	0.8	0.7	0.7

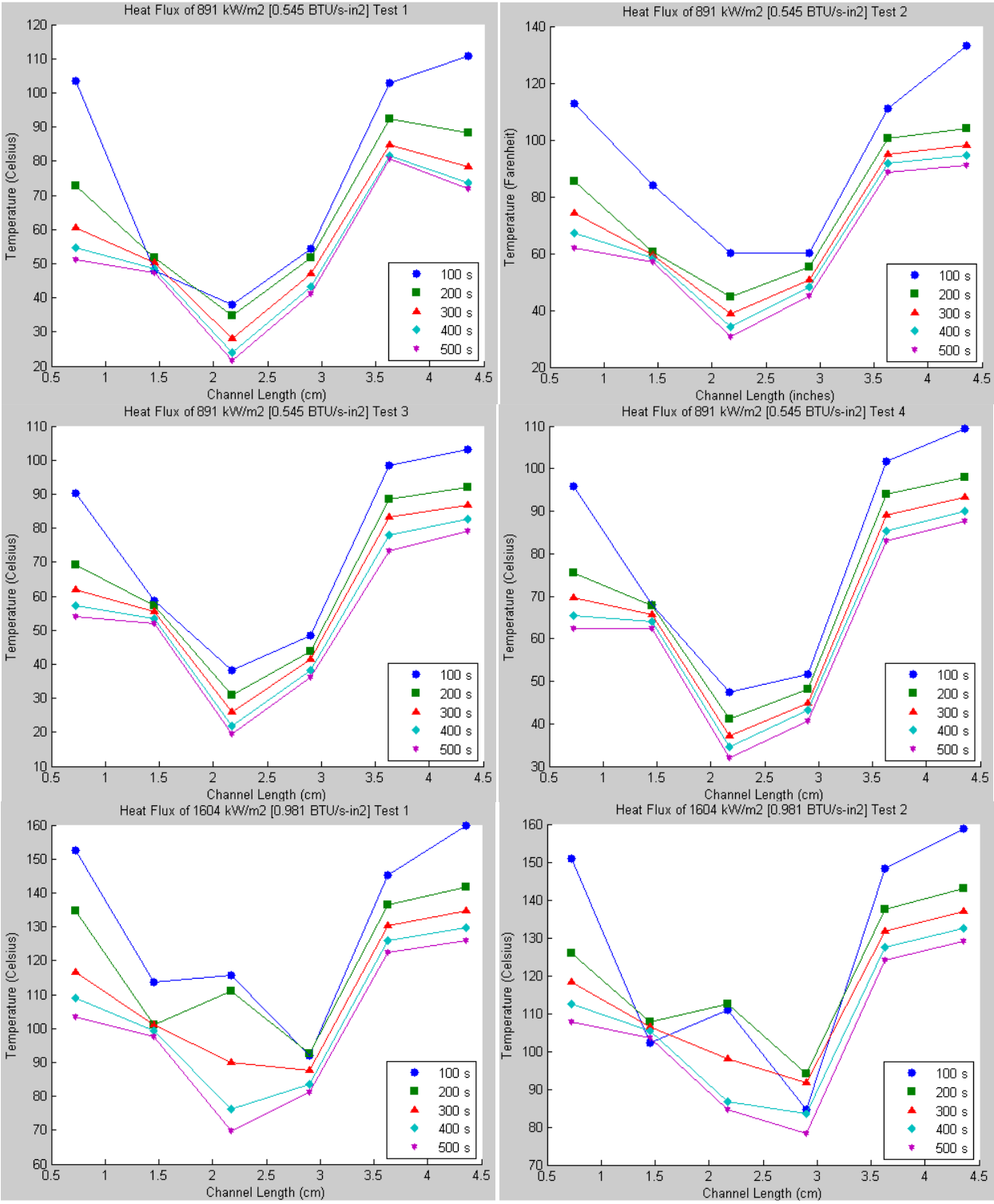

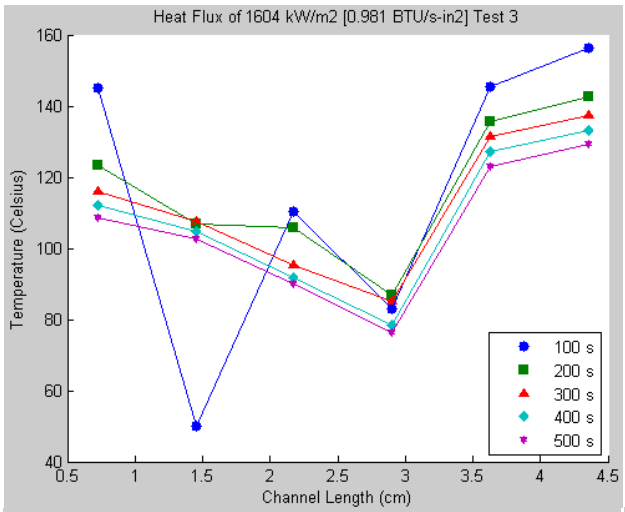
Heat Flux of 1604 kW/m2 [0.981 BTU/s-in2] Test 3
Temperature (Celsius)
Channel Length (cm)
100 s
200 s
300 s
400 s
500 s

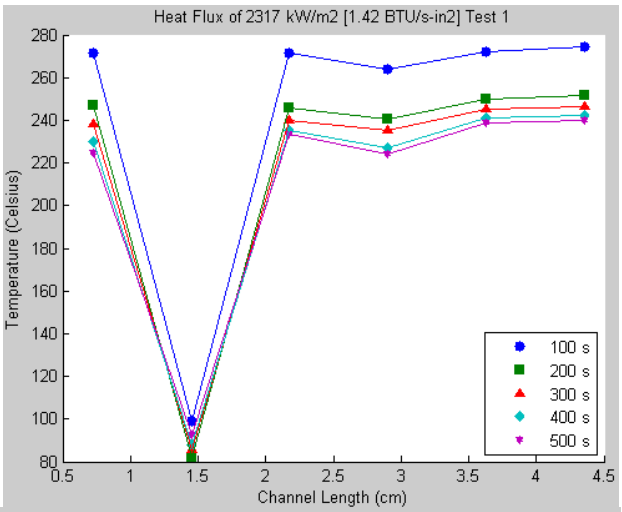
Heat Flux of 2317 kW/m2 [1.42 BTU/s-in2] Test 1
Temperature (Celsius)
Channel Length (cm)
100 s
200 s
300 s
400 s
500 s

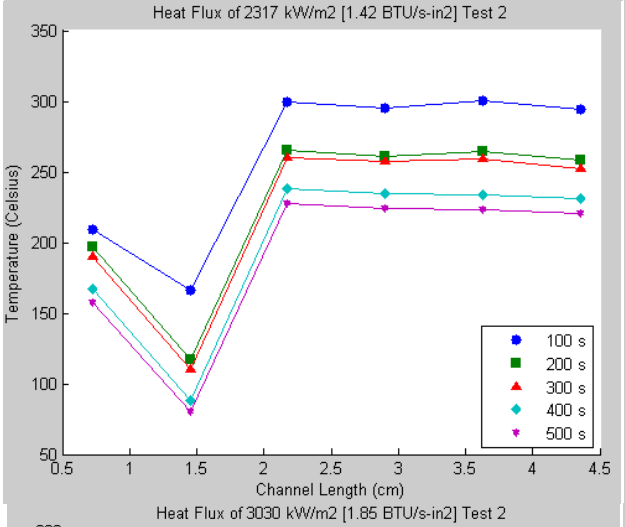
Heat Flux of 2317 kW/m2 [1.42 BTU/s-in2] Test 2
Temperature (Celsius)
Channel Length (cm)
100 s
200 s
300 s
400 s
500 s

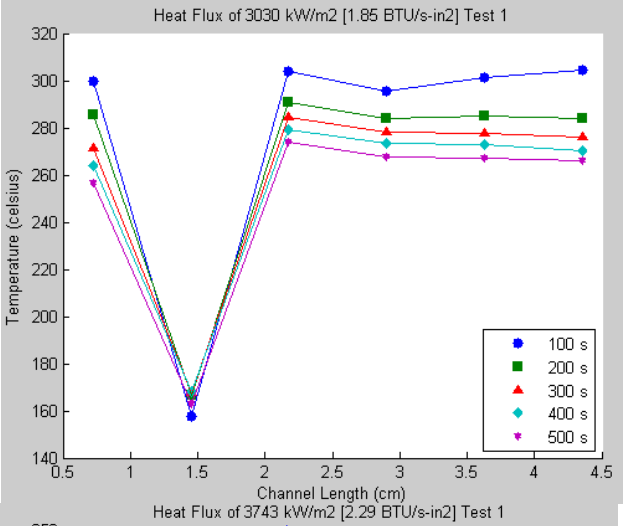
Heat Flux of 3030 kW/m2 [1.85 BTU/s-in2] Test 1
Temperature (Celsius)
Channel Length (cm)
100 s
200 s
300 s
400 s
500 s

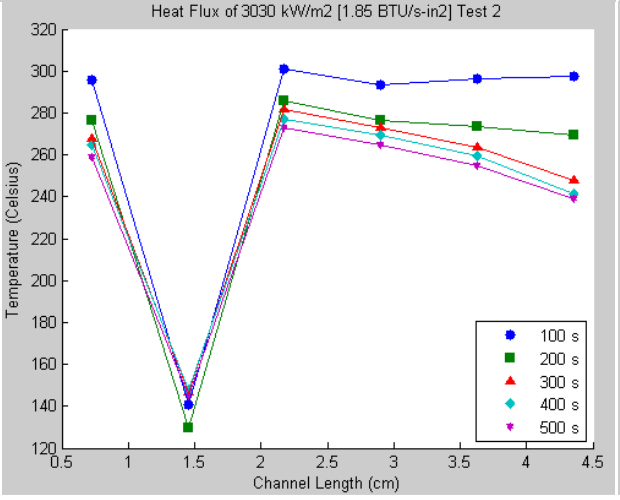
Heat Flux of 3030 kW/m2 [1.85 BTU/s-in2] Test 2
Temperature (Celsius)
Channel Length (cm)
100 s
200 s
300 s
400 s
500 s

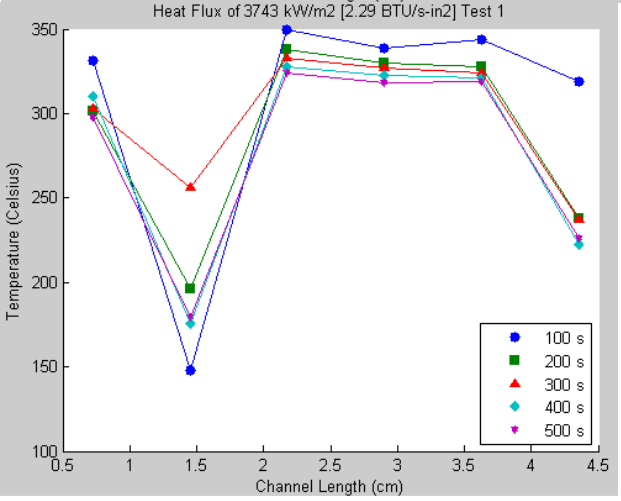
Heat Flux of 3743 kW/m2 [2.29 BTU/s-in2] Test 1
Temperature (Celsius)
Channel Length (cm)
100 s
200 s
300 s
400 s
500 s

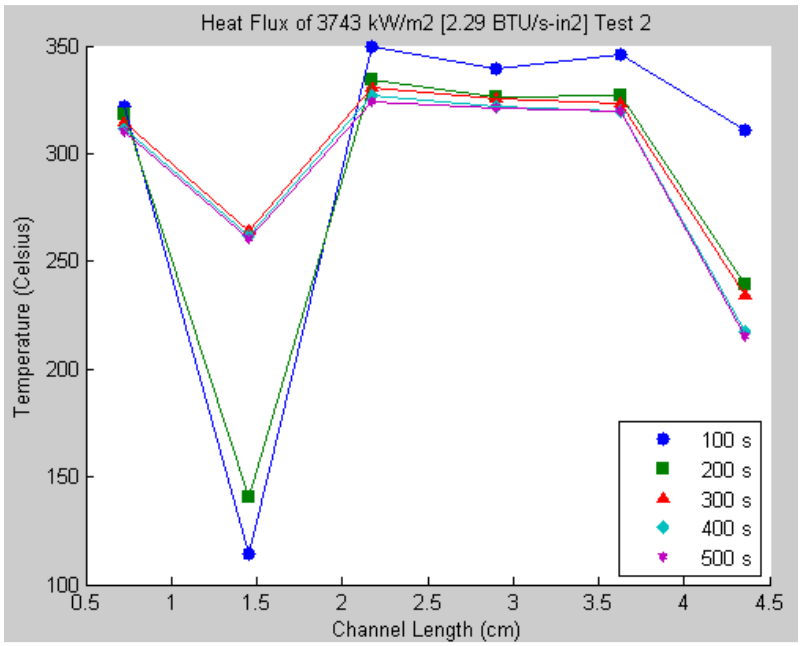

Appendix D: Channel Wall Temperature with Distance Plots Normalized

(+/-) Error (°C)					
TC1	TC2	TC3	TC4	TC5	TC6
0.8	0.9	1	0.8	0.7	0.7

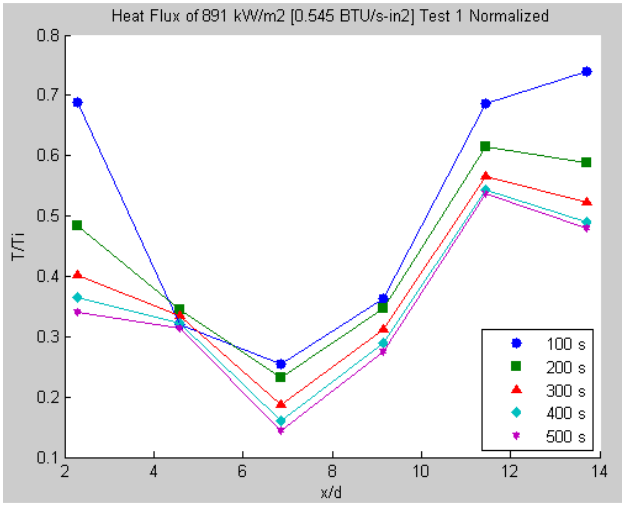

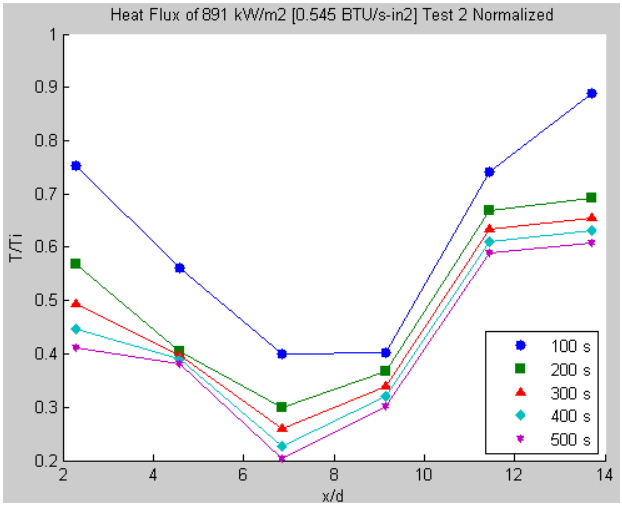

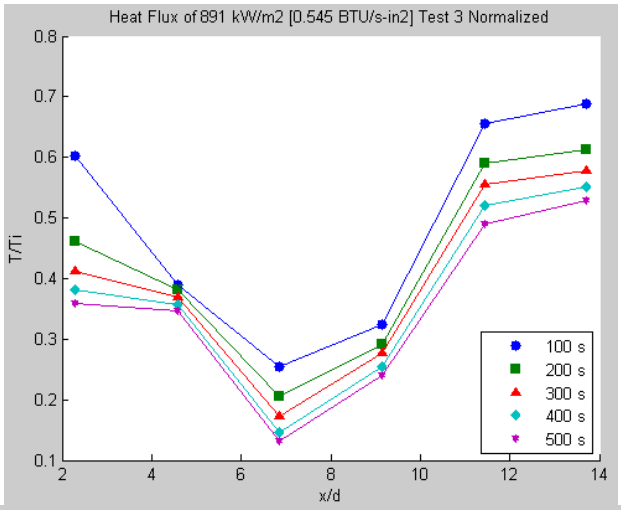
Heat Flux of 891 kW/m2 [0.545 BTU/s-in2] Test 3 Normalized
T/Ti
x/d
100 s
200 s
300 s
400 s
500 s

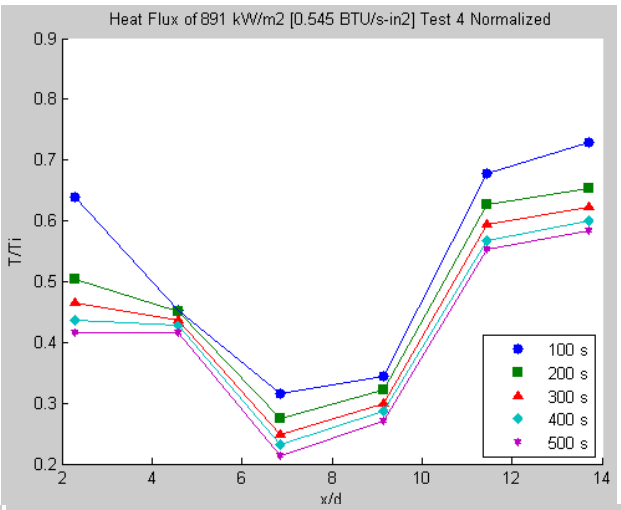
Heat Flux of 891 kW/m2 [0.545 BTU/s-in2] Test 4 Normalized
T/Ti
x/d
100 s
200 s
300 s
400 s
500 s

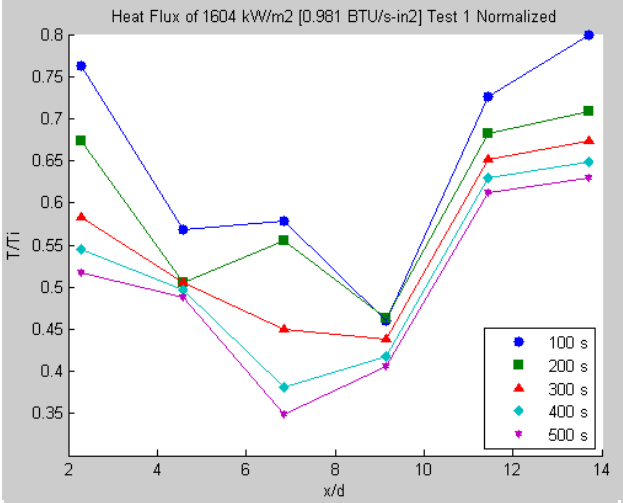
Heat Flux of 1604 kW/m2 [0.981 BTU/s-in2] Test 1 Normalized
T/Ti
x/d
100 s
200 s
300 s
400 s
500 s

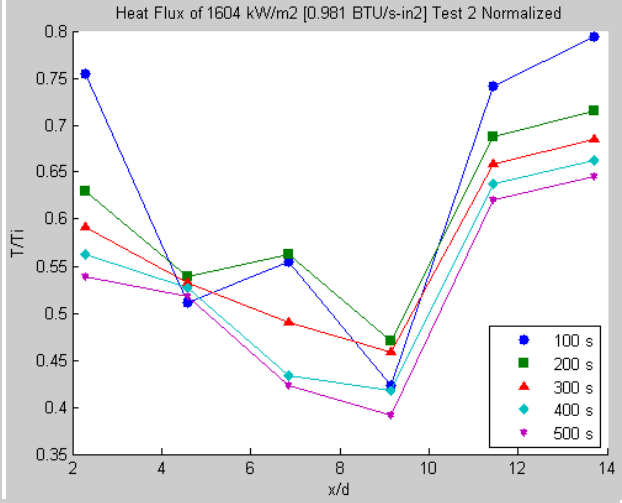
Heat Flux of 1604 kW/m2 [0.981 BTU/s-in2] Test 2 Normalized
T/Ti
x/d
100 s
200 s
300 s
400 s
500 s

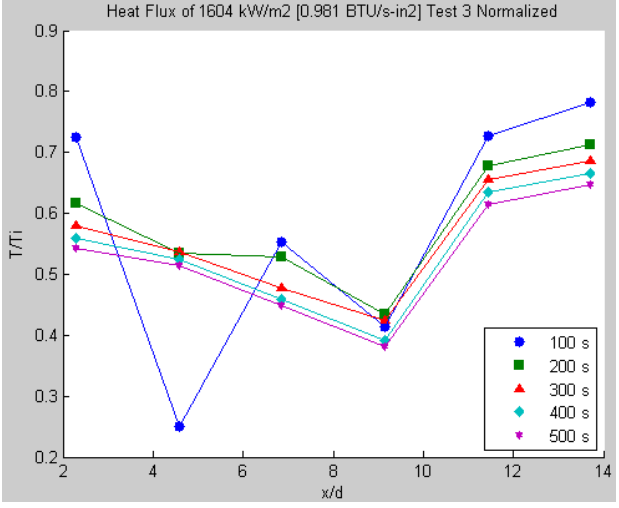
Heat Flux of 1604 kW/m2 [0.981 BTU/s-in2] Test 3 Normalized
T/Ti
x/d
100 s
200 s
300 s
400 s
500 s

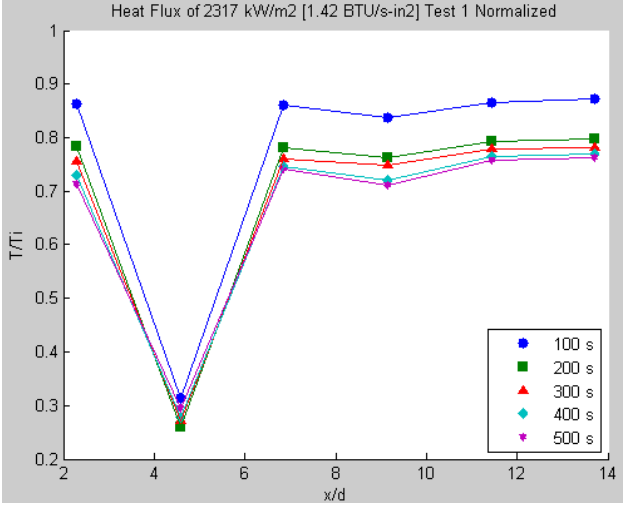
Heat Flux of 2317 kW/m2 [1.42 BTU/s-in2] Test 1 Normalized
T/Ti
x/d
100 s
200 s
300 s
400 s
500 s

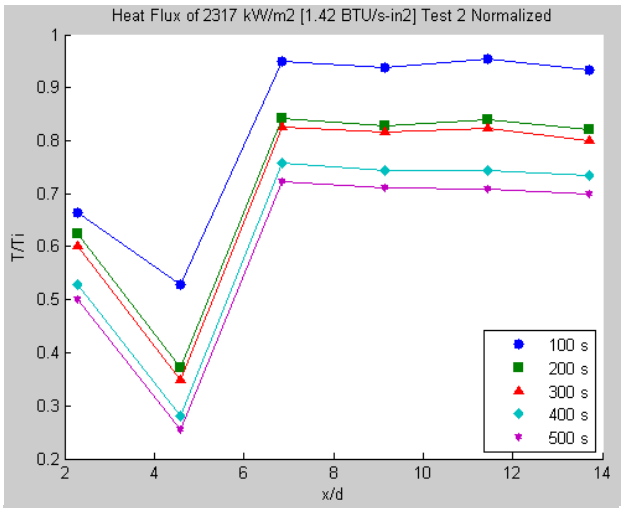
Heat Flux of 2317 kW/m2 [1.42 BTU/s-in2] Test 2 Normalized
T/Ti
x/d
100 s
200 s
300 s
400 s
500 s

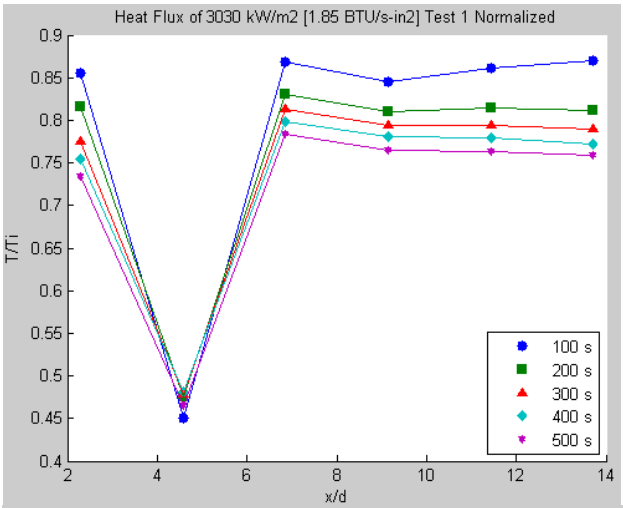
Heat Flux of 3030 kW/m2 [1.85 BTU/s-in2] Test 1 Normalized
T/Ti
x/d
100 s
200 s
300 s
400 s
500 s

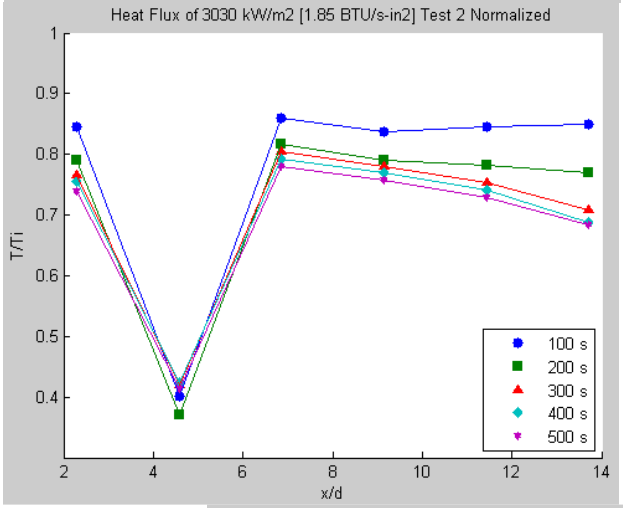
Heat Flux of 3030 kW/m2 [1.85 BTU/s-in2] Test 2 Normalized
T/Ti
x/d
100 s
200 s
300 s
400 s
500 s

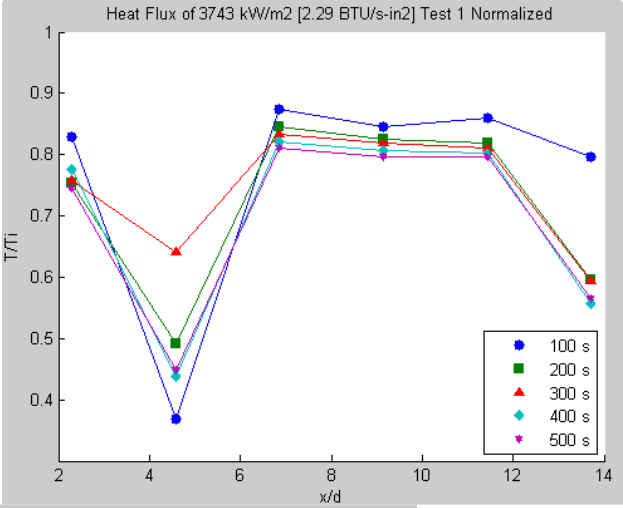
Heat Flux of 3743 kW/m2 [2.29 BTU/s-in2] Test 1 Normalized
T/Ti
x/d
100 s
200 s
300 s
400 s
500 s

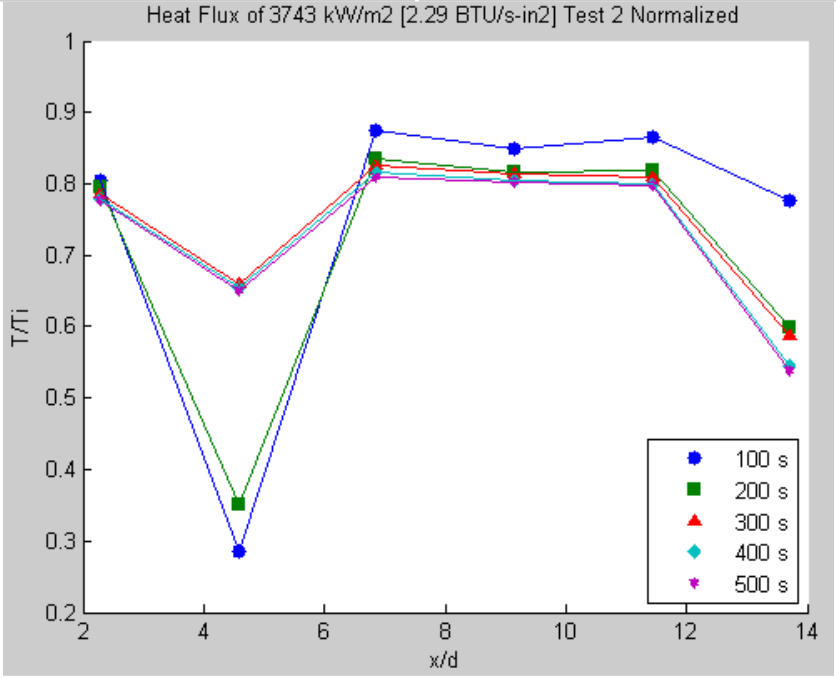
Heat Flux of 3743 kW/m2 [2.29 BTU/s-in2] Test 2 Normalized
T/Ti
x/d
100 s
200 s
300 s
400 s
500 s

Appendix E: Liquid Methane Tests

(+/-) Error (°C)					
TC1	TC2	TC3	TC4	TC5	TC6
0.8	0.9	1	0.8	0.7	0.7

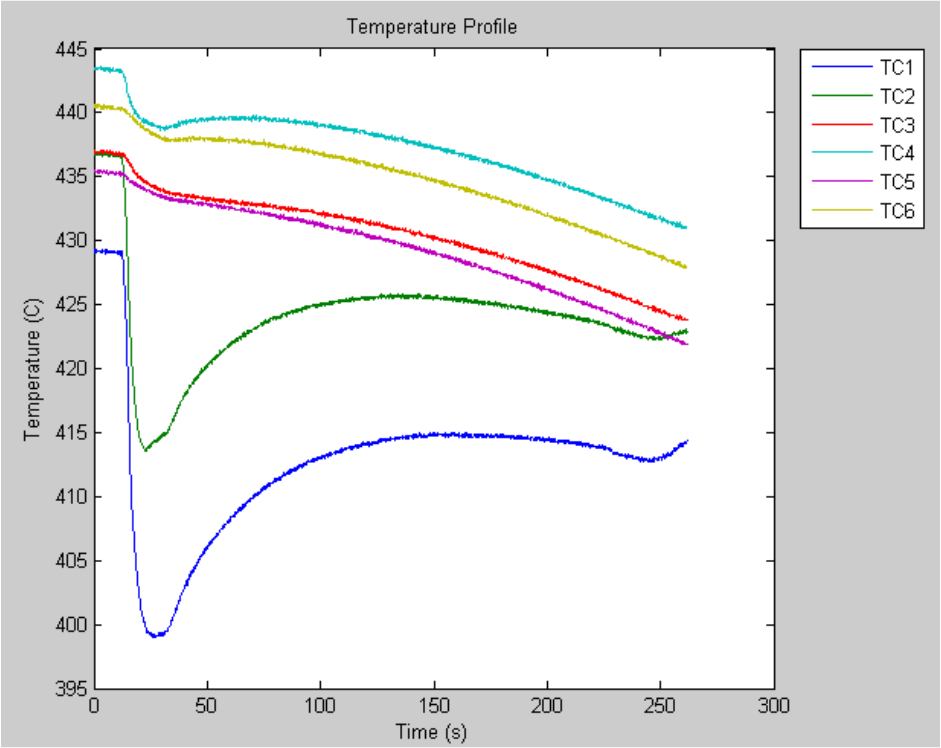

First test with LCH_4 with heat flux of 3743 kW/m^2

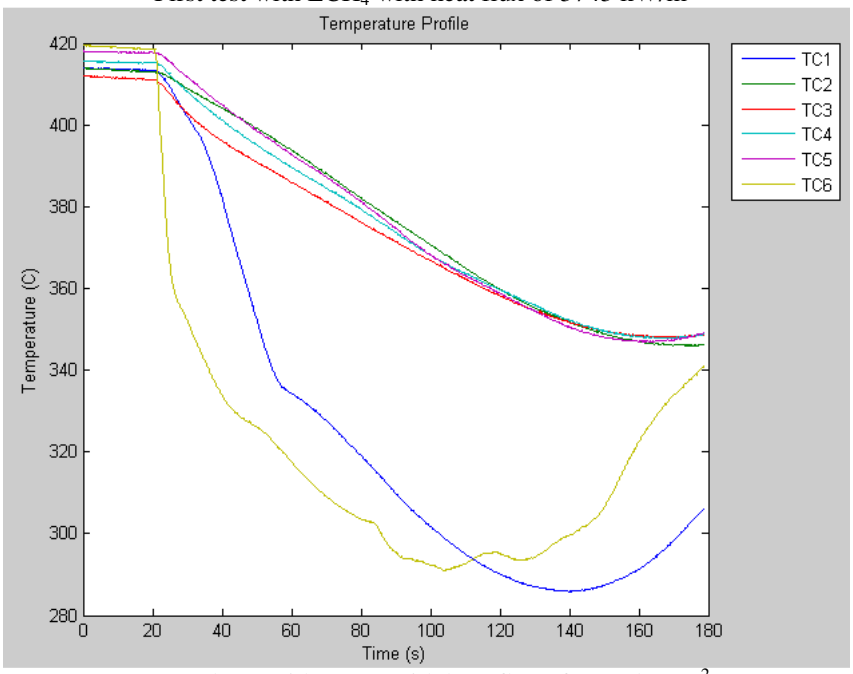

Second test with LCH_4 with heat flux of 3743 kW/m^2

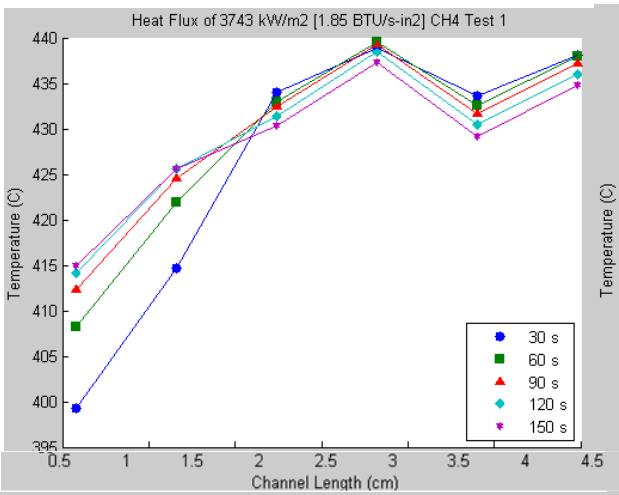
Heat Flux of 3743 kW/m2 [1.85 BTU/s-in2] CH4 Test 1
Temperature (C)
Channel Length (cm)
30 s
60 s
90 s
120 s
150 s

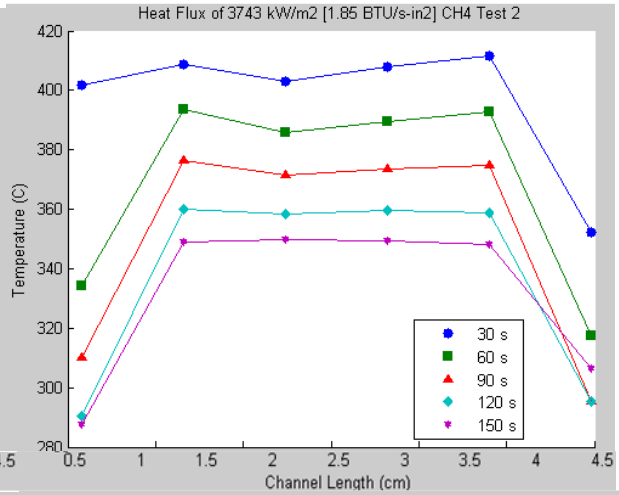
Heat Flux of 3743 kW/m2 [1.85 BTU/s-in2] CH4 Test 2
Temperature (C)
Channel Length (cm)
30 s
60 s
90 s
120 s
150 s

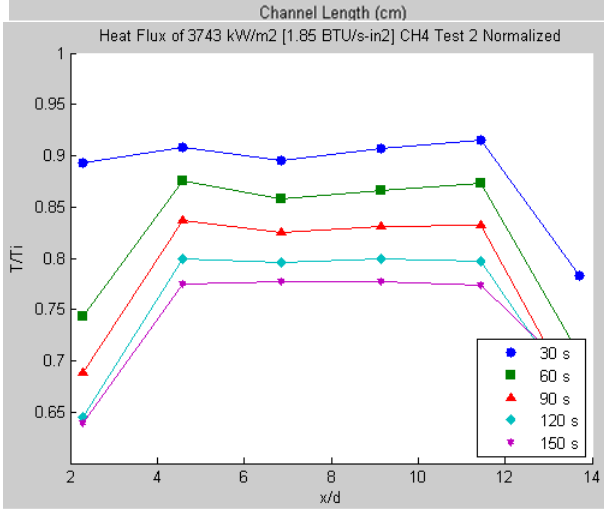
Heat Flux of 3743 kW/m2 [1.85 BTU/s-in2] CH4 Test 2 Normalized
T/Ti
x/d
30 s
60 s
90 s
120 s
150 s

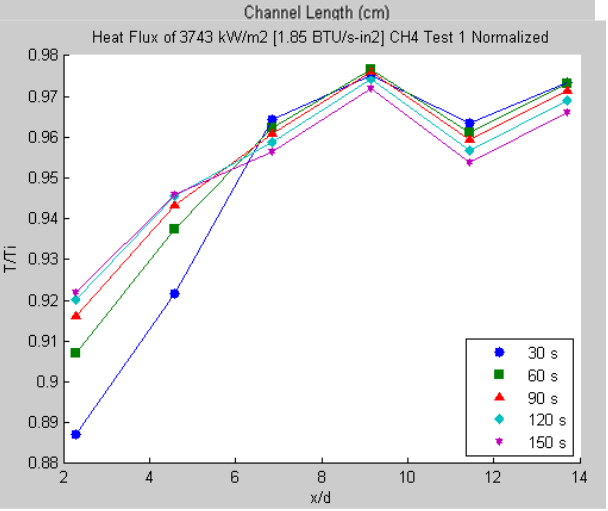
Heat Flux of 3743 kW/m2 [1.85 BTU/s-in2] CH4 Test 1 Normalized
T/Ti
x/d
30 s
60 s
90 s
120 s
150 s

CURRICULUM VITAE

Sergio Flores was born on September 18, 1986 in El Paso, Texas to Sergio A. and Mercedes Flores. He graduated high school as Salutatorian in 2005 from Bel Air High School in El Paso, Texas. Sergio later received his Bachelor of Science in Architectural Engineering in the spring of 2009 from The University of Texas at Austin. During his undergraduate degree he worked as an undergraduate research assistant with the Texas Research Experience program and he interned with Sandia National Laboratories in the summer of 2008 with the Wind Energy Department. After his undergraduate degree Sergio pursued his Master of Science in Civil Engineering at The University of Texas at El Paso where he worked as a Teaching Assistant in Graphic Design and a Research Assistant for the Center of Space Exploration and Technology Research (cSETR). During his Master's Sergio worked at the cSETR under Dr. Ahsan Choudhuri.

Permanent Address: 472 Borrett St.
El Paso, Texas 79907

This thesis was typed by Sergio Flores.